THE ZONE PLATE INTERFEROMETER

by

Raymond Newton Smartt

Submitted in Partial Fulfillment

of the

Requirements for the Degree

MASTER OF SCIENCE

Supervised by Professor Brian J. Thompson

The Institute of Optics
The University of Rochester
Rochester, New York

1970

ACKNOWLEDGEMENT

The author wishes to express his gratitude to Dr. Brian J. Thompson for his advice and encouragement during the preparation of this thesis.

ABSTRACT

This thesis develops the basic idea of a Fresnel zone plate two-beam interferometer[1], leading to a description of what is undoubtedly a very useful and practical instrument.

In the introductory chapter, the elements of two-beam interference and partial coherence are presented. To add some perspective to later discussion, the main features of some well known two-beam interferometers are briefly reviewed and compared. Representative examples of the 'common-path' class of designs - the scatter plate interferometer and a birefringent design - are also described. Murty's proposal for a Fresnel zone plate, common-path, interferometer is then discussed.

The zone plate interferometer in its developed form is described in detail, and three basic configurations, or modes, of the interferometer are distinguished, associated with the real and virtual first order foci of the zone plate. These modes are treated systematically and analyzed, and their respective advantages and disadvantages given. Multiple diffraction orders give rise to multiple configurations - and multiple interference patterns. These possibilities are also discussed.

The classical Fresnel zone plate and its modified forms are reviewed and their properties given. An interferometric method to prepare phase type zone plates,

including a means to generate uniform amplitude wavefronts, is described. Moiré fringes allow the accuracy of the zone plates to be measured in a simple manner.

A zone plate interferometer has been constructed and its description is given in detail. This includes component specifications, the method of alignment, and the location of fringes. The results obtained using a zone plate in different modes, and the phenomenon of compound interference patterns are discussed and interpreted particularly from the viewpoint of holography.

A comparison has been made between the performance of this interferometer and a compact Twyman-Green interferometer. Interferograms which illustrate this test are included, revealing the high quality of the interference pattern (close to unit visibility) with the zone plate instrument.

Possible errors intrinsic to the interferometer system are also examined. It is shown that self-compensation reduces most of these to a negligible value.

The zone plate interferometer is simple to construct and to operate, and is a useful addition to the range of common-path designs; perhaps, in many respects, the most useful.

TABLE OF CONTENTS

TABLE OF CONTENTS (cont'd)

LIST OF FIGURES

LIST OF FIGURES (cont'd)

INTRODUCTION

Common-path interferometers have a number of attractive features compared with other two-beam interferometers. For example, intrinsically they have relatively stable and high contrast interference patterns. The advantages stem from the chief characteristic of common-path designs - that is the reference and test beams have equal optical paths along a common axis. Examples of these interferometers are the wave shearing types, the scatter plate interferometer, and some polarization forms.

A different type of common-path interferometer has been suggested, and its feasibility demonstrated, by Murty[1], It employs a Fresnel zone plate which has the function of a diffracting beam-splitter to provide the required beams. The optical system which Murty gives is similar to that shown elsewhere for the scatter plate interferometer[2], suggesting that it may be considered simply as a variant of the latter and that a zone plate may be regarded in this application as a circularly symmetric scatter plate. The analogy does not extend very far however, and while the scatter plate interferometer has been developed and indeed is generally favored (at the present time) to test components such as large telescope objectives, no report of any development of the zone plate interferometer has appeared in the literature. It appears therefore that no sound basis for

this preference exists.

The work which this thesis describes commenced as an independent investigation of the possible application of zone plates to two-beam interferometers and a simple interferometer was designed without acquaintance with the first paper cited above. The discovery of this earlier work stimulated more interest in the possibilities of development of this device, and further analysis revealed many intriguing aspects of its operation. The results of this analysis - the multiple configurations, the high quality of performance, and the potential of this interferometer - are treated in detail in this thesis.

I. TWO-BEAM INTERFEROMETRY

1.1 Coherence and Interference

These topics, as related to two-beam interference, will be introduced first from a qualitative point of view to establish basic concepts.

An optical source is termed coherent if the radiation which it emits has a waveform characterized by a pure sinusoid with respect to time. This is an idealized concept, most closely approached by a single frequency laser.

Two beams of radiation are (mutually) coherent if the phase difference between them is constant during the period normally covered by observations. This allows the possibility of statistical fluctuations of phase in each source, or equivalently in each beam. Two beams are incoherent when the phase difference changes many times and in a random way during the shortest period of observation; that is, the statistical fluctuations are uncorrelated. It is the intermediate condition of partial coherence which is of practical interest.

1.1.1 Time coherence and spatial coherence

The interference pattern produced by a two-beam interferometer is a cosinusoidal variation of intensity when expressed as a function of the path difference p or the time difference $\tau = p/c$ of the two beams. Where the radiation has a range of frequencies $\Delta\nu$, the intensity is proportional to the integral taken over this range. It is in fact still

cosinusoidal, but the modulation decreases as the time difference increases. This condition is expressed in the uncertainty relation

$$\Delta\tau\,\Delta\nu \sim 1 \quad ,$$

where $\Delta\tau$ is called the coherence time. The corresponding coherence length is then

$$\Delta p = c\Delta\tau \quad .$$

Spatial coherence is related to the effective angular source size. Consider a hypothetical point source. The time dependence of any two field points equally distant from the source will be precisely the same; that is, the fields at these points are mutually coherent. For an incoherent source with some spatial extension however, the fields are no longer completely coherent.

If the source subtends a solid angle $\Delta\Omega$, for light of mean wavelength λ_o, and two field points with a separation Δl, an 'area of coherence' $(\Delta l)^2$ is expressed by

$$(\Delta l)^2\,\Delta\Omega \sim \lambda_o^2 \quad .$$

1.1.2 Two-beam interference

Consider two effective sources situated at points P_1 and P_2 with complex (scalar) amplitudes represented by $A_1(P_1,t)$ and $A_2(P_2,t)$. At a point P where the radiation from the two sources is superimposed, the complex amplitude is

$$A(P,t) = A_1(t) + A_2(t+\tau) \quad ,$$

where τ is the time difference for the two paths. The net amplitude and phase of $A(P,t)$ may vary with time in a random

fashion, depending on the properties of the two sources, and when this occurs, correspondingly, the instantaneous intensity will fluctuate rapidly. The observable quantity is the time averaged intensity I(P) given by

$$I(P) = \langle A(P,t)A^*(P,t)\rangle$$
$$= \langle A_1 A_1^*\rangle + \langle A_2 A_2^*\rangle + 2\mathrm{Re}\left[\langle A_1^*(t)A_2(t+\tau)\rangle\right]$$
$$= I_1 + I_2 + 2\mathrm{Re}\left[\Gamma(P_1,P_2,\tau)\right] \quad ,$$

where $\Gamma_{12}(\tau) = A_1^*(t)A_2(t+\tau)$ is called the 'mutual coherence function'. This may be normalized to give the dimensionless 'degree of coherence'

$$\gamma_{12}(\tau) = \frac{\Gamma_{12}(\tau)}{\sqrt{\Gamma_{11}(0)\Gamma_{22}(0)}} = \frac{\Gamma_{12}(\tau)}{\sqrt{I_1 I_2}} \quad ,$$

and the intensity is then,

$$I(P) = I_1 + I_2 + 2\sqrt{I_1 I_2}\ \mathrm{Re}\left[\gamma_{12}(\tau)\right] \quad .$$

$\gamma_{12}(\tau)$ is in general a periodic function of τ. We can write,

$$\gamma_{12}(\tau) = \left|\gamma_{12}(\tau)\right| e^{i\theta(\tau)} \quad ,$$

where $\theta(\tau)$ is the argument of the complex quantity $\gamma_{12}(\tau)$, and for a mean frequency ν_o,

$$\theta(\tau) = \alpha(\tau) + 2\pi\nu_o\tau \quad .$$

Then

$$\mathrm{Re}\left[\gamma_{12}(\tau)\right] = \left|\gamma_{12}(\tau)\right| \cos\left[\alpha(\tau) + 2\pi\nu_o\tau\right] \quad .$$

Now the degree of coherence satisfies the relation

$0 \leq |\gamma_{12}(\tau)| \leq 1$, and we have

$|\gamma_{12}| = 1$ complete coherence

$|\gamma_{12}| = 0$ complete incoherence

$0 < |\gamma_{12}| < 1$ partial coherence .

For an interference pattern, the intensity then varies between the limits,

$$I_{max} = I_1 + I_2 + 2\sqrt{I_1 I_2}\,|\gamma_{12}| \quad ,$$

$$I_{min} = I_1 + I_2 - 2\sqrt{I_1 I_2}\,|\gamma_{12}| \quad .$$

The fringe visibility V(P) is defined as

$$V = \frac{I_{max} - I_{min}}{I_{max} + I_{min}} \quad ;$$

or,

$$V = \frac{2\sqrt{I_1 I_2}\,|\gamma_{12}|}{I_1 + I_2} \quad .$$

For the zone plate interferometer, I_1 and I_2 are always approximately equal, and since the path difference $p = c\tau$ is at the most of the order of wavelengths only, $|\gamma_{12}| \approx 1$, and a visibility close to unity can be expected.

In many interferometers, however, stray light in the interference field significantly reduces the effective value of V.

1.2 Twyman-Green Interferometer

This interferometer will now be discussed briefly to add some perspective to the description of common-path interferometers to follow. It typifies the 'earlier' types of interferometers and therefore is a useful example to consider.

Referring to Fig. 1, the interferometer is adjusted to operate in parallel light with the monochromatic point source S at the principal focus of the collimating lens L_1. A second

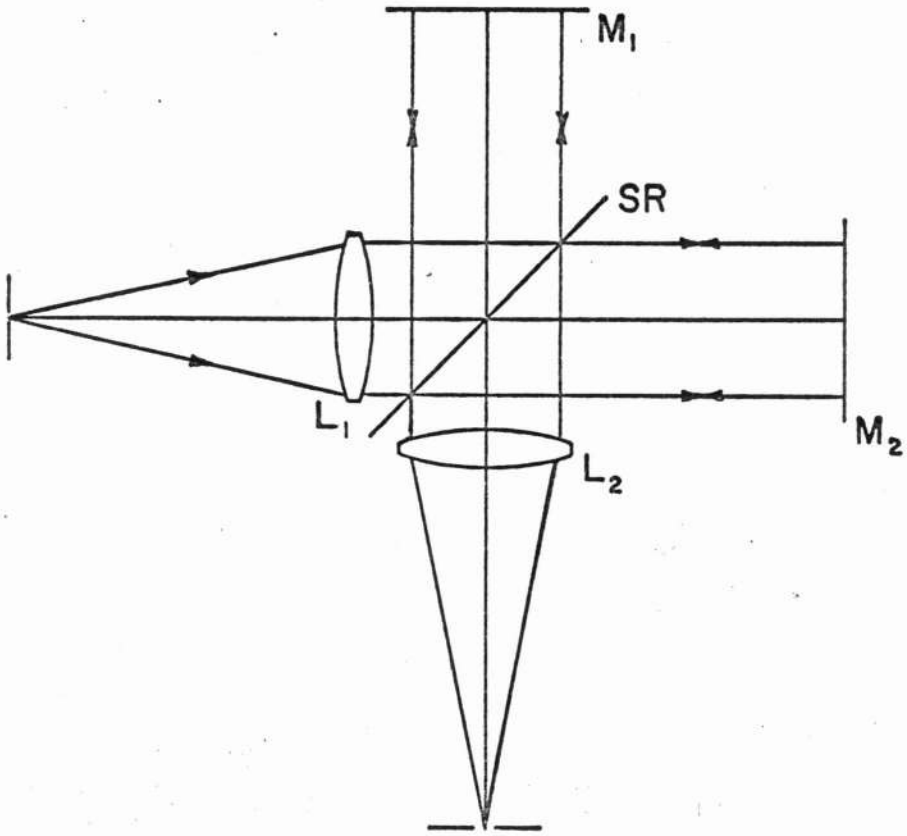

Fig.1. Twyman-Green Interferometer. SR, semi-reflector; M_1, M_2, plane mirrors; L_1, collimating lens; L_2, viewing lens.

lens L_2 focuses the emergent light into the plane of observation. The fringes are localized approximately in the plane of the mirrors. When the image of mirror M_1, say, is adjusted to be parallel to the plane of the mirror M_2, the field is uniform. This interference pattern will pass through one cycle when one of the mirrors is translated parallel to itself through half a wavelength. This follows from the double passage of the light in the two arms of the interferometer, and characterizes most two-beam interferometers. Note that if a piece of glass with slightly inclined surfaces is placed in one arm of the interferometer (adjusted for a uniform background interference field), consecutive fringes represent one wavelength increments in glass thickness for an index of 1.5.

The Twyman-Green interferometer is a versatile instrument. A prism may be tested for surface defects and inhomogeneities in the glass by inserting it in one arm, and tilting the mirror to return the light along the same path. With auxiliary optics, lenses and mirrors may also be tested. For example, a collimating lens may be tested by positioning the lens in one arm, and replacing the plane mirror in that arm with an accurately spherical convex mirror of appropriate radius of curvature.

There are some unattractive features however. Compensation may be difficult to achieve where the system under test has a significantly large optical thickness. The amplitudes

of the two interfering components and their states of polarization are unlikely to match due to the properties of typical beam-splitters. A compensating plate is necessary if a white light source is used. Since the arms are separated in this interferometer, it is very sensitive to vibration and air turbulence. In its normal form, the apertures of the mirrors and beam-splitter must at least equal that of the component under test, so that it becomes a very expensive instrument to construct, and is limited in the size of optics that can be tested. Its ultimate accuracy depends of course on the precision with which the mirrors and beam-splitter are constructed.

A compact form of the Twyman-Green interferometer has been described[3], appropriate for use with a laser source. The reference arm is then typically an external surface of the beam-splitter-prism and there is therefore no question of matching paths. When used to test a lens or concave mirror, the interferometer aperture can be left quite small. A lens system in the test arm is then used to generate a diverging spherical wavefront. This system must be highly corrected of course. For a laser source operating in more than one cavity mode, the fringe visibility may approach zero where the path difference is equal to the laser cavity length or odd multiples of it.

1.3 Lateral Shearing Interferometer

The lateral shearing interferometer is also mentioned here since it stands as a unique concept and is favored for many applications. Originally described by Bates[4], it exists in a number of forms, such as the Mach-Zehnder configuration represented in Fig. 2a, and the far simpler system in Fig. 2b, the latter appropriate for use only with a laser source since the paths do not match. To test a concave mirror, an optical system similar to that used typically in other two-beam interferometers is employed to provide a divergent spherical wavefront. The fundamental difference here is that the beam is divided after leaving the test arm. No reference beam is involved in this system, the two interfering wavefronts being derived from the simple process of laterally shearing the wavefront emerging from the test arm with itself. Obvious advantages are that it is not necessary to produce an accurate reference wavefront (in this respect it is an absolute measurement), and that the interference system is extremely stable. Nevertheless, since only the gradient of the aberration (for small shear) is revealed in the interferogram, the usefulness of this interferometer is necessarily limited. This property also means that any analysis of an interferogram to determine the wavefront shape must be carried through two stages, each of which can affect the accuracy of the determination.

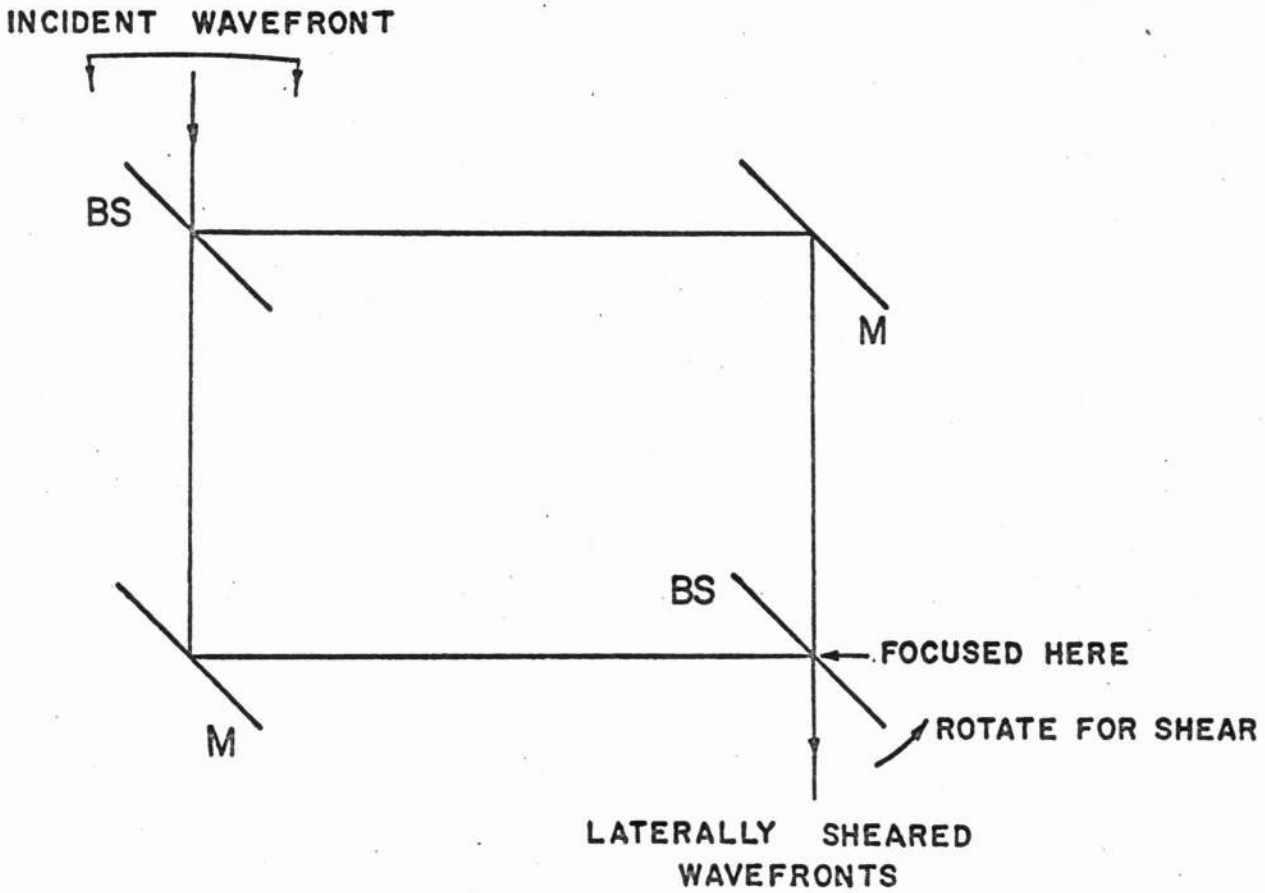

Fig. 2a. Lateral Shearing Interferometer (Mach-Zehnder configuration). BS. beam-splitter; M, plane mirror. (Figures 2a, 2b, 3, 4 and 5, are based on those given in the Institute of Optics paper, 'A Description of Various Test Procedures for Evaluating Quality of Large Optics', by M. Murty).

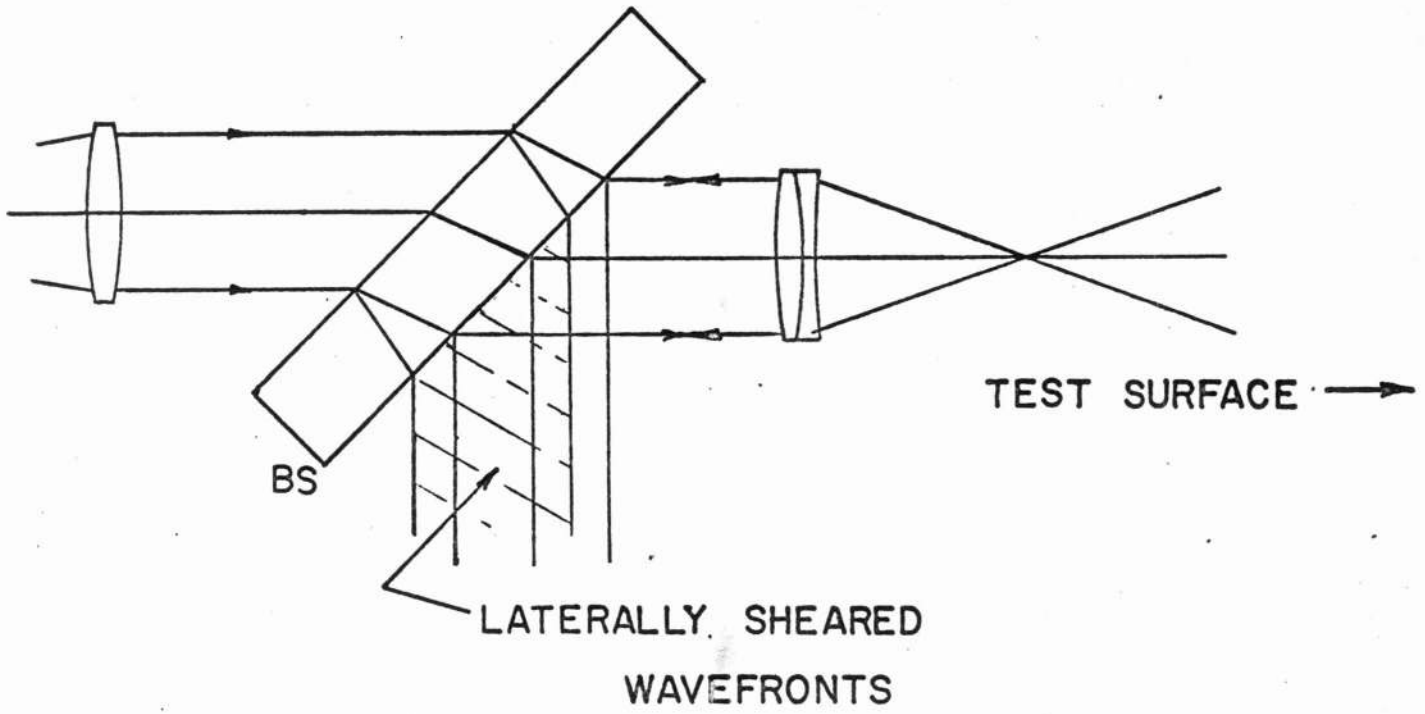

Fig.2b Lateral Shearing Interferometer (fixed shear). BS, glass beam-splitter.

This interferometer is intermediate in form between a design such as the Twyman-Green interferometer where the divided components follow separate paths, and the common-path interferometers where the axial paths are equal. The latter are discussed in the following section.

1.4 Common-path Interferometers

These interferometers[5] have several favorable properties compared with other two-beam interferometers. Advantages stem from the distinguishing characteristic of common-path designs -- the reference and test beams have equal optical paths along a common axis. It follows that thermal fluctuations in the air path, will, at least to some extent, affect both beams in a similar way; that is, phase variations impressed on each beam will be partly correlated, dependent on the relative beam diameters. Since the interferometer measures phase difference, the magnitude of such disturbances as registered in the interference pattern will be diminished. Partial compensation of the effect of vibration also will occur where both beams pass through the same optics and are reflected at the same surfaces. A stable interference pattern is therefore typical of this class of interferometer and fringe visibility is substantially independent of the reflectance of the system under test.

Belonging to the common-path class of interferometers are the 'double focus' interferometers[6] in which the reference

beam forms an image of the source at the system under test, while the test beam expands to fill the test aperture. A concave optical surface or lens can be tested simply in this way and the full wave-aberration obtained directly from the interferogram. Examples of double focus interferometers are the scatter-plate interferometer[2], and several polarization designs[6].

Dyson has described a common-path polarization interferometer (a double focus design) which uses a compound birefringent lens, as indicated in Fig. 3. Incident polarized light gives rise to two orthogonally polarized components. The lens is designed to have zero power for one component, and this can then be independently focused at the surface of the mirror to supply a reference beam. The other component emerges from the lens as a divergent wavefront to function as the test beam. The planes of polarization of the two components are interchanged after passing twice through a quarter wave plate, producing matching wavefronts of the interfering components. In common with similar designs, this interferometer, though convenient to use, is difficult and expensive to manufacture, depending critically in performance on the quality of the birefringent lens. The multiple optical surfaces are likely to cause troublesome images when used with a laser source.

Even more novel is the scatter plate interferometer[2], also a double focus design. In practice a scatter plate

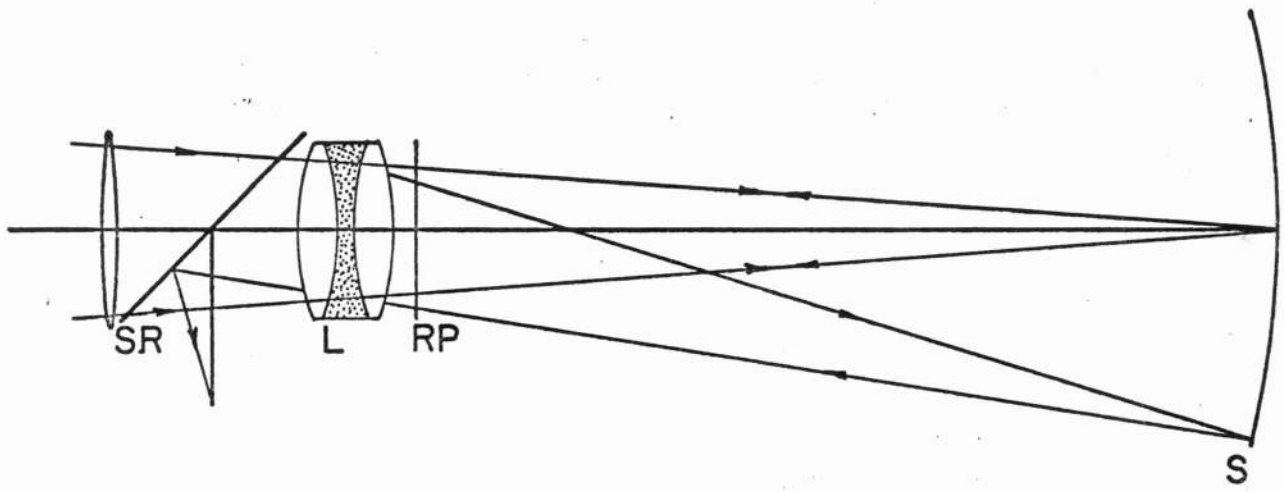

Fig.3 Common-path Polarization Interferometer. L, compound birefringent lens; RP, $\lambda/4$ retardation plate; S, surface under test; SR, semi-reflector.

transmits more light directly than is scattered or diffracted, and it is this direct light which is focused by an auxiliary lens onto the surface under test, to form, as before, a reference beam. A system using two scatter plates is represented in Fig. 4. That part of the diffracted light which is reflected by the mirror to the second scatter plate is the test beam, and interference occurs in this plane. The light which passes directly through both scatter plates forms a bright image in the center of the field. The plate SP_2 is coincident with the virtual image of the first plate SP_1, and accurately orientated so that a scattering point on SP_1 corresponds to an identical scattering point on SP_2. Otherwise an interference pattern cannot be obtained, or, with only slight misalignment, the fringes have reduced visibility.

In the developed form of this interferometer[8], only one scatter plate is used, prepared in such a manner that it has radially symmetrical properties; that is, there is a center of symmetry. This is achieved in the following way. A photographic plate is exposed to a collimated beam of light from a laser source, with a ground glass surface almost in contact with the photographic emulsion. A second exposure is then made, but with the ground glass rotated through precisely 180°. The performance of the interferometer depends critically on the degree to which symmetry is preserved[8].

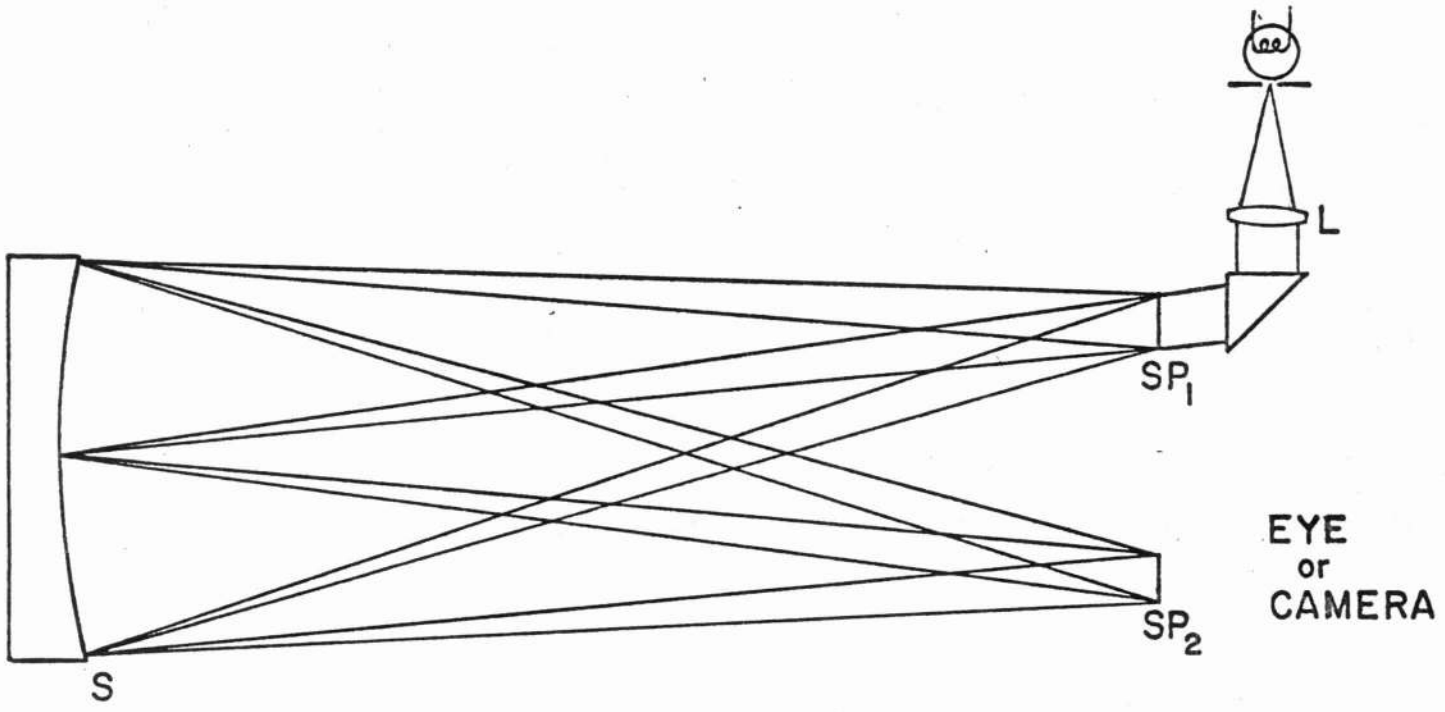

Fig.4 Scatter Plate Interferometer. SP_1, SP_2, identical scatter plates; S, surface under test; L, positive lens to focus the source at the test surface.

1.4.1 Common-path interferometer using Fresnel zone plates

While linear diffraction gratings have been used in conventional interferometers to replace beam-splitters and mirrors, the idea of using Fresnel zone plates as beam-splitters to form a common-path double focus interferometer is due to Murty[1]. This proposal will now be discussed.

Murty's scheme is represented in Fig. 5. Light from either a broad band or monochromatic source, passing through the circular aperture A, is focused by the lens L to form an image of A at the center of the surface S under test. This is the reference beam of the interferometer. Portion of the incident light is diffracted at the zone plate ZP_1, the center of which is offset laterally from the center of curvature of the surface S. The diffracted light constitutes the test beam and diverges to fill the aperture of S, so that the reflected light forms an image of ZP_1 at the second zone plate ZP_2, co-planar with ZP_1. The centers of the zone plates ZP_1 and ZP_2 are therefore positioned symmetrically about the center of curvature of S. At the second zone plate, some of the diffracted light (the test beam) passes through as a direct beam while some of the direct light is diffracted. These two beams are the interfering components.

The author makes no distinction between the plus and minus orders or between the first and higher orders, although both plus and minus first orders are represented (apparently)

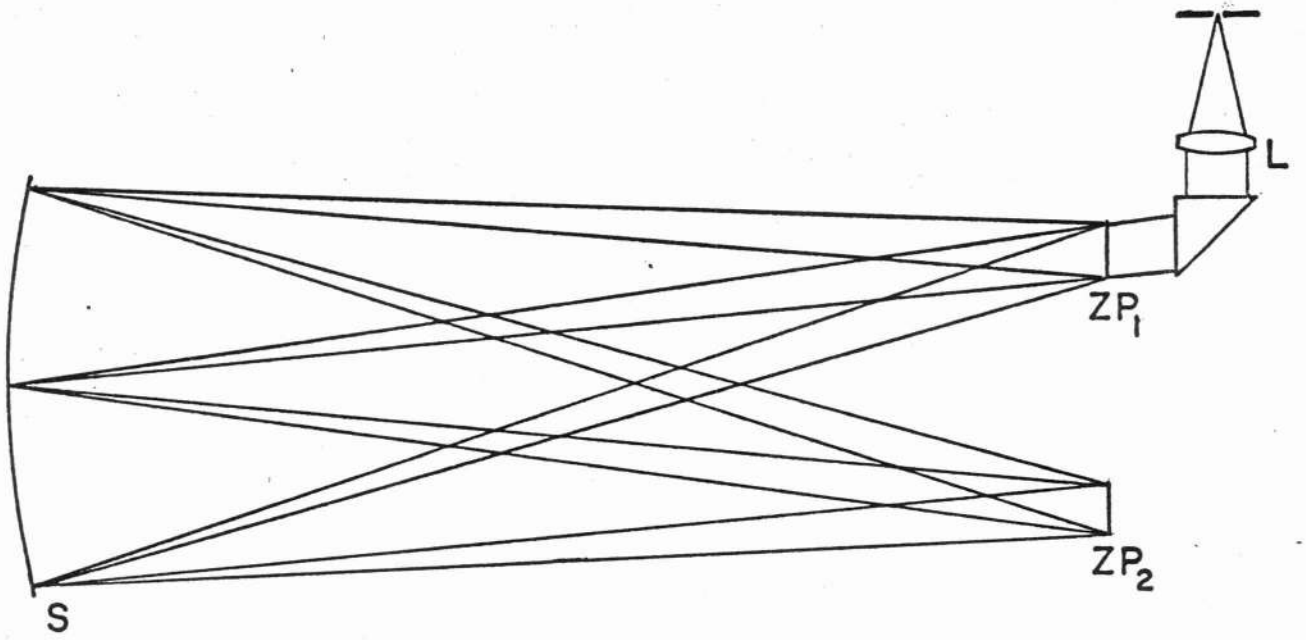

Fig.5 Fresnel Zone Plate Interferometer (configuration due to Murty). ZP_1, ZP_2, identical zone plates; S, surface under test; L, positive lens used to focus the source at the test surface.

in Fig. 5, taken from the paper. Various interferograms are given which demonstrate the feasibility of the system. Each contains a bright central spot, typical also of the scatter-plate interferometer, which the author of the paper attributes to "that part of the beam of light which is not diffracted by either plate plus a portion of the light which is diffracted by both plates." (It will be shown later that this undesirable feature of the interference pattern can be eliminated.) Note that since path differences are small by definition of a common path system, temporal coherence is not necessary and a white light source can be used.

The author states that an interferometer using zone plates is an alternative system to the scatter-plate interferometer. It is therefore not surprising that a configuration which uses two zone plates is presented, identical with that given previously for the scatter-plate interferometer. But a zone plate, unlike a scatter-plate, is circularly symmetric and it is an overall advantage to use only one zone plate.

Zone plates of 3mm aperture and a primary focal length of 52mm (f/17) were used. These were Fresnel zone plates, being photographic negatives of a drawing of a Fresnel zone system. The arrangement for the interferometer to test a lens with an infinite conjugate (in combination with a plane mirror) is also given in the paper, as well as the equivalent system where the plane mirror is replaced by an identical system to that preceding the mirror.

This paper[1] stands as the presentation of a novel idea -- that Fresnel zone plates can in principle be used to form a common-path interferometer - supported by some evidence to verify that an interference pattern can be obtained, as well as suggestions for its exploitation. It is perhaps surprising that there has been no further development along these lines reported in the literature.

II. ZONE PLATE INTERFEROMETER DESIGNS

The proposal which Murty[1] has made to construct a common-path interferometer based on a Fresnel zone plate has been discussed in the first chapter. This idea will now be developed in a general manner and extended to show that different configurations are possible, leading to the complete description of a practical interferometer.

2.1 Basic Principle of Operation

A Fresnel zone plate has lens-like properties with multiple foci forming real and virtual images. It is the conjugate relationship between these images - the generation of identical wavefronts from different incident beams - which allows a zone plate to be used as the basis of a double-focus interferometer, where the zero and first diffraction orders most conveniently provide the required two beams. More specifically, the zero order light, which passes without diffraction through the zone plate, constitutes the reference beam while the first order diffracted light becomes the test beam. After reflection and a second passage through the zone plate, the first order component of the reference beam and the zero order component of the test beam combine to give an interference pattern in which consecutive fringes represent half-wavelength increments in single passage optical path. Since each beam is diffracted

only once in its double passage through the zone plate, the interfering components have approximately equal amplitudes. Interference arising from combinations which include other orders will be considered also.

Two degrees of freedom are required - one for each beam. These are the position of the zone plate along the axis with respect to the system under test and the position of the source image formed by the reference beam. It will become evident in the following discussion that for each configuration these two requirements are simultaneously satisfied. More explicitly, consider a test surface in a fixed position along the optical axis. The test beam is focused by a lens to form an image of the source either at the test surface or at infinity, while the zone plate can then be moved independently along the axis to give the correct condition for the test beam.

2.2 Interferometer Configurations

An obvious simplification of the design given by Murty is to use only one zone plate rather than two, as discussed in Chapter I. A partial-reflector must then be introduced into the system to observe the interference pattern. But the use of one zone plate demands that it have precise radial symmetry since an entering ray may, depending on the configuration, leave the system at a diametrically opposite point. Otherwise a wavefront error would result from the

lack of symmetry. These points are discussed in detail in this and later chapters. Also, as shown in Chapter III, it is not necessary to draw a Fresnel zone system and then photographically copy this to obtain a suitable zone plate, but simply to photograph an appropriate interference pattern - a far simpler procedure - so that f/1 zone plates can be made rather than the example of f/17 quoted by Murty. Other modifications lead to greater light efficiency, an absence of the typical bright spot in the center of the interference field and close to uniform amplitude in both wavefronts. These will all be dealt with in detail in the following chapter.

To test a concave mirror or similar system, the zone plate interferometer can be set up in a number of different ways. In fact, as will now be demonstrated, the proposal already discussed to use two zone plates (or the equivalent one zone plate form) represents only a small part of the total possibilities for this interferometer. It turns out that this design is actually one of three distinct (but equivalent) configurations. These different configurations will now be designated 'modes' of the interferometer. In turn, each mode exists in different versions. We may differentiate between the alternative modes on the basis of the position of the zone plate in relation to the center of curvature of the mirror. These are where the center of curvature coincides with:

1. the center of the zone plate
2. a virtual focus of the zone plate
3. a real focus of the zone plate .

What are the coherence requirements for the source radiation? These modes are all common-path systems, and for zero tilt, the axial paths of the reference and test beams are equal (zero delay). In fact, for a spherical mirror at focus, all paths are equal. It follows that temporal coherence is not essential, and a broad band or even white light source can be used. The situation is not as simple with regard to spatial coherence. The second and third modes (for a convergent reference wavefront) each have one of the two interfering wavefronts laterally inverted with respect to the other. It is therefore necessary that the source size (actual or effective) be sufficiently small that spatial coherence exists across the entire field. For a circular incoherent source of radius r, the degree of partial coherence between two laterally separated field points P_1, P_2, is given by

$$\left|\gamma_{12}(0)\right| = \left|\frac{2J_1(Z)}{Z}\right| ,$$

where $J_1(Z)$ is the Bessel function of the first order,

$$Z = \frac{2\pi rd}{\lambda_o R} ,$$

d is the distance separating P_1 and P_2, R is the source distance, and λ_o is a representative wavelength. Consider an example where d, measured in the plane of the zone plate, has a value of 1cm, R is 10cm, and λ_o is 550nm. If a degree

of partial coherence equal to 0.8 is taken as an acceptable lower limit, then the radius of the source r required to satisfy this condition is

$$r \approx 1.5\ \mu m \ .$$

This is such a small value that of conventional sources, high pressure arc lamps alone would be suitable, and points to the considerable practical advantage of a laser source.

It is convenient to classify the set of diffracted components for any incident beam which form real images the plus orders, denoted by (+1,+2,---), and virtual images the minus orders, or (-1,-2,---). That part of the incident light which is transmitted directly by the zone plate is then a zero order, or (0).

2.2.1 Mode 1

In mode 1, the center of the zone plate coincides with the center of curvature of the mirror under test. Such a system is indicated in Fig. 6. An image of the source is formed at the center of the surface of the mirror by the projection lens L_1. This beam then remains unaberrated by any macroscopic irregularities of the test surface and functions as the reference beam. The test beam is a minus first order, or (-1), component (of a convergent incident beam), which after reflection and a second passage through the zone plate gives rise to a zero order, or (-1,0), beam. This divergent wavefront and that from the (0,-1) reference beam combine to form the required interference pattern. Light

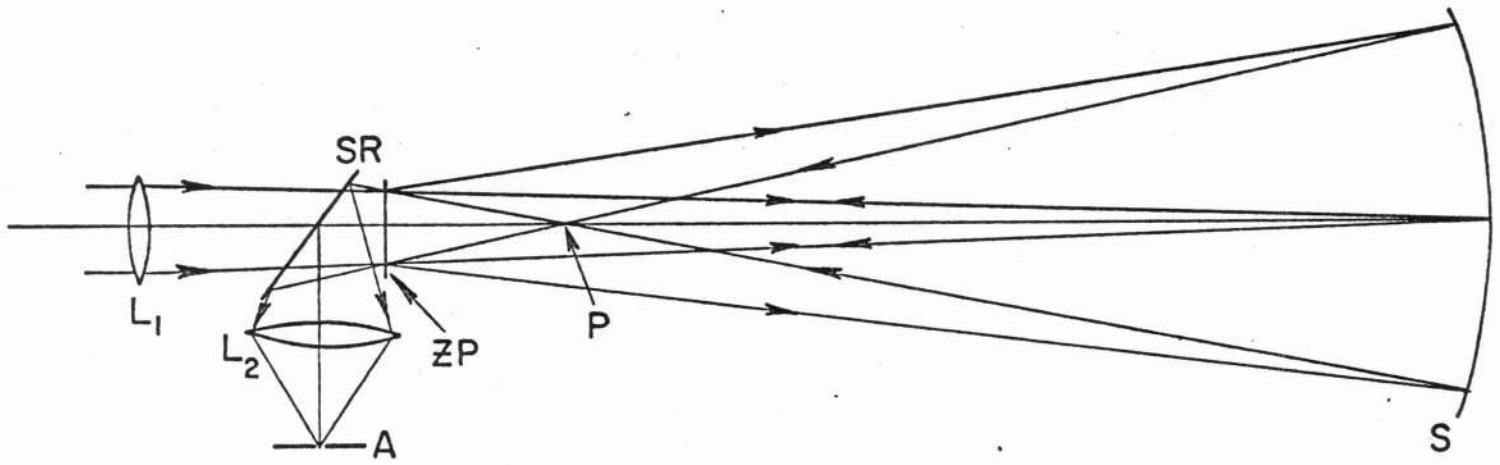

Fig.6 Zone Plate Interferometer in mode 1. ZP, zone plate; SR, semi-reflector; S, surface under test; L_1, positive lens to focus the source at the test surface; A, small aperture which functions as a selective field stop; L_2, positive lens to focus the two interfering wavefronts in the plane of A; P, simultaneous focal point for the (-1) component after reflection and the (+1) component.

from other order combinations will also be present in the interference field. Conveniently, the lens L_2 in combination with the aperture A (typically a hole 0.5mm or less in diameter) serves to exclude this extraneous light almost completely from the interferogram.

There is, however, a second beam combination possible in this mode, producing another interference pattern which carries identical information. This arises in the following way. By symmetry considerations, it can be seen that the point of intersection of the rays reflected from the spherical surface, labeled P in Fig. 6, is also the (+1) component focus. This component then defines another test beam, in which the light travels in the reverse direction to that indicated in Fig. 6 appropriate for the previous case. The interference pattern is a combination of a (+1,0) test beam and a (0,+1) reference beam. These are convergent wavefronts and the lens L_2 therefore may be omitted from this system. For a zone plate having a primary focal length f, and a mirror of radius of curvature R, the point P lies at a distance Rf/(R+f) from the zone plate.

Fig. 7 is a compound interference pattern consisting of three identical sets of fringes, without L_2 and A present in the system. The largest set arises from the first case cited; the next set from the second case. The inner set is reversed in phase with respect to the other two patterns and is a special case since it appears as a single interference pattern only

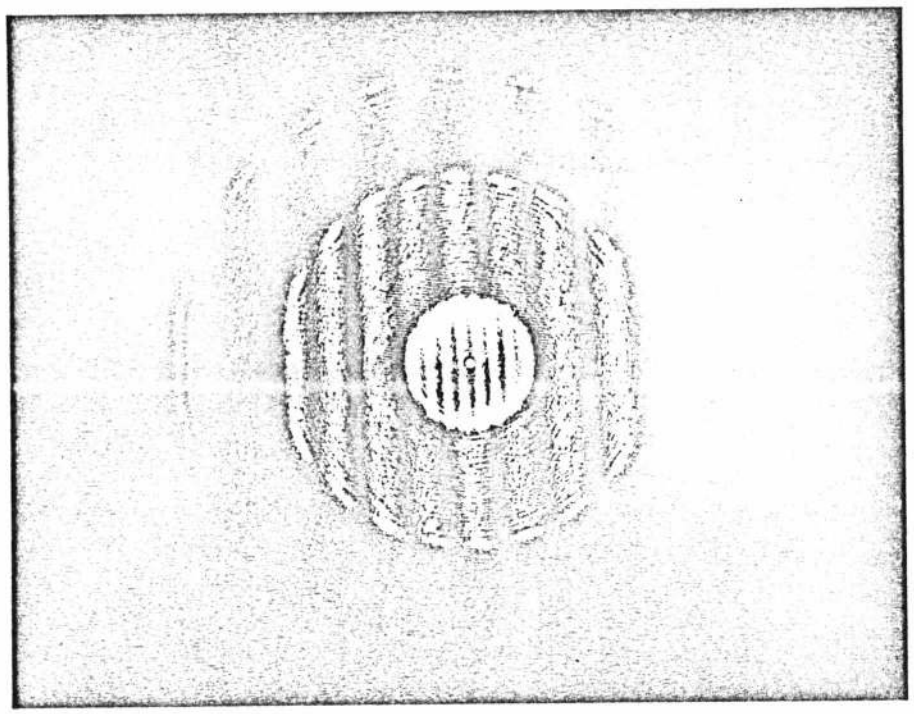

Fig. 7. Compound Interference Pattern. This is observed in the mode 1 configuration without the aperture A in the system.

when the zone plate is at the center of curvature. The two test beams distinguished above, following reflection at the concave surface, each have a diffracted component into the (0,0) beam cone. Fringes of this center set, having moderate visibility, then result from the combination of this doubled test beam and the (0,0) reference beam. Yet again, a smaller set of fringes, not evident in this interferogram, may be observed. These have a similar origin to the second set, except that on the second pass through the zone plate, the next higher order (+1 increment) components are involved, to give a (+1,+1) test beam and a (0,+2) reference beam. Each beam has thus been diffracted through the same number of orders. Depending on the properties of the zone plate, this combination can still result in wavefronts with approximately equal amplitudes.

A still smaller set of fringes can be found and so on, and then in turn a set larger than the largest set evident here. In fact any pair of beams for which this condition applies, that is reference and test wavefronts diffracted into the same beam and with equal amplitudes, will also have an associated family of interference patterns in higher orders. These patterns will generally be faint where the higher orders are weak. In this mode, the finite effective aperture of the zone plate (determined by its primary focal length and the test aperture) means that the surface under test is not tested strictly at its center of curvature. As

shown by Scott[8], for a similar type of optical configuration using a scatter-plate, in typical tests the resultant error is negligible.

2.2.2 Mode 2

In Fig. 8, a second mode for the interferometer is represented which occurs when the zone plate is moved closer to the test surface such that the first order virtual focus is coincident with the center of curvature of the mirror. The useful interference pattern here is derived from a (0,+1) reference beam and a (-1,0) test beam. Conveniently, these beams are convergent. Since one beam is laterally reversed with respect to the other after reflection, a laser source is particularly appropriate. Also, the interference pattern is more sensitive to centering and alignment of the zone plate and any aberrations of the incident beam which lack axial symmetry. Errors due to such causes are negligible using normal optical alignment procedures. Referring again to Fig. 8 note that while the reference beam may be aberrated in its path through the lens L_1 and partial reflector R, so also, in this common-path system will the test beam. To a first order approximation, therefore, any such aberrations which have axial symmetry will cancel.

2.2.3 Mode 3

The zone plate may be moved further from the system under test than either of the previous configurations. For this third mode (Fig. 9), the first order real focus coincides

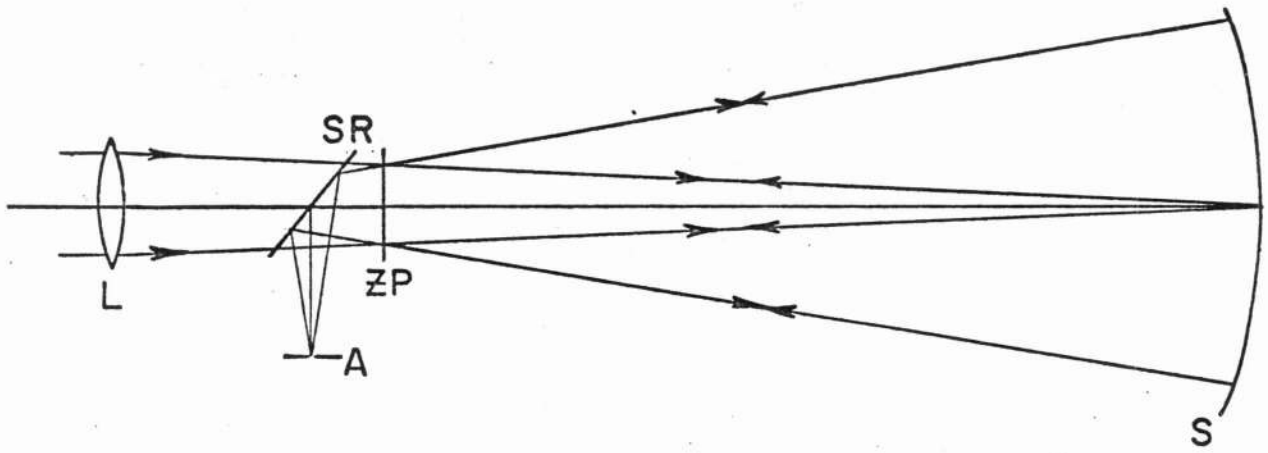

Fig. 8. Zone Plate Interferometer in mode 2. ZP, zone plate; SR, semi-reflector; S, surface under test; A, small aperture.

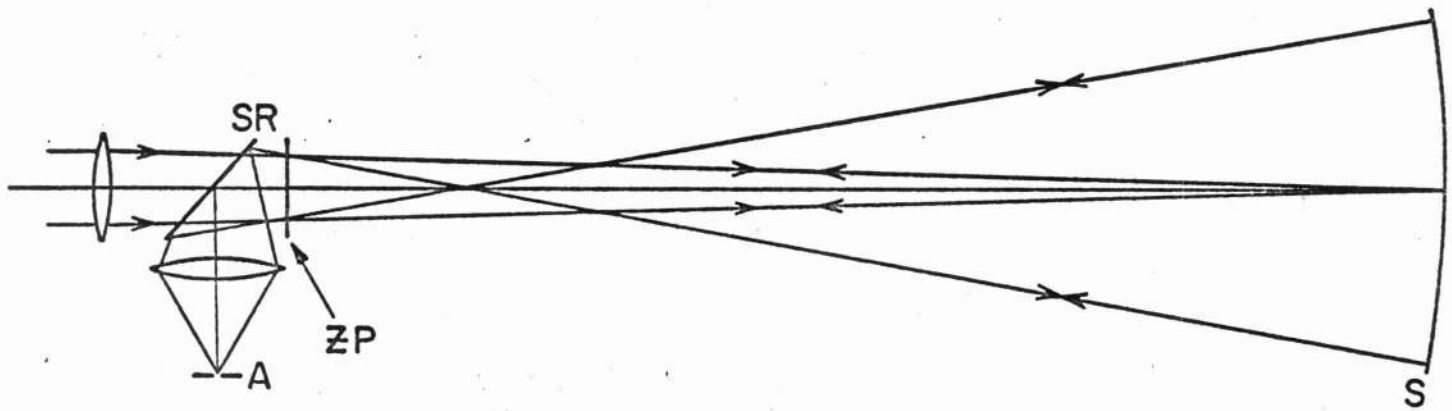

Fig. 9. Zone Plate Interferometer in mode 3. ZP, zone plate; SR, semi-reflector; S, surface under test; A, small aperture.

with the center of curvature of the mirror. The divergent fringe system then arises from a (0,-1) reference beam and a (+1,0) test beam. Again there is no aperture restriction on the zone plate, but one wavefront is laterally reversed with respect to the other.

In each of the above cases, fringes are easily obtained by bringing to coincidence any of the appropriate pairs of images. Note that although the three modes are equivalent in terms of the information given in the corresponding interferograms, the first mode alone can be used with white light, while the second and third test truely at the center of curvature.

2.2.4 Alternative versions

Three modes of the zone plate interferometer have been described, classified according to the position of the zone plate in relation to the center of curvature of the system under test. Equivalently, the classification could have been on the basis of the three different configurations of the test beam. In each case the reference beam incident on the test surface is the same. But this is not the only possibility, and a second version of each mode follows by choosing a different reference beam. That is, instead of focusing the source at the test surface, it is focused at infinity. The three configurations for the test beams remain the same, but the reference beam is now collimated within the interferometer proper. A plane mirror is required,

centered on axis and close to the plane of the test surface, to auto-collimate the reference beam. The second mode of the interferometer in this version is shown in Fig. 10. (The other two modes are not shown since their configurations are obvious from this example.) Referring to Fig. 10, the lens L_1 now functions as a collimating lens, and a plane wavefront is incident on the zone plate. The reference beam is, as before, a zero order of the zone plate, and emerges from the zone plate after reflection from the mirror as a (0,+1) beam. It combines with the (-1,0) test beam to produce an interference pattern. This is not a double-focus design as in the other version, nor even, strictly, a common-path interferometer if set up as shown in the figure, since the paths are not equal. Nevertheless, most of the advantages of the common-path class are retained.

Perhaps this configuration might be considered of little practical interest since a plane reflector is required and part of the test surface is obscured. There are some attractive features, however. Well-corrected collimating lenses are commonly available, and such a component can be chosen for the lens L_1, which is set with one infinite conjugate for all tests. The partial reflector, now in collimated light, introduces no aberration, and since the zone plate was constructed using a plane wavefront, with collimated light incident, the zone plate func-

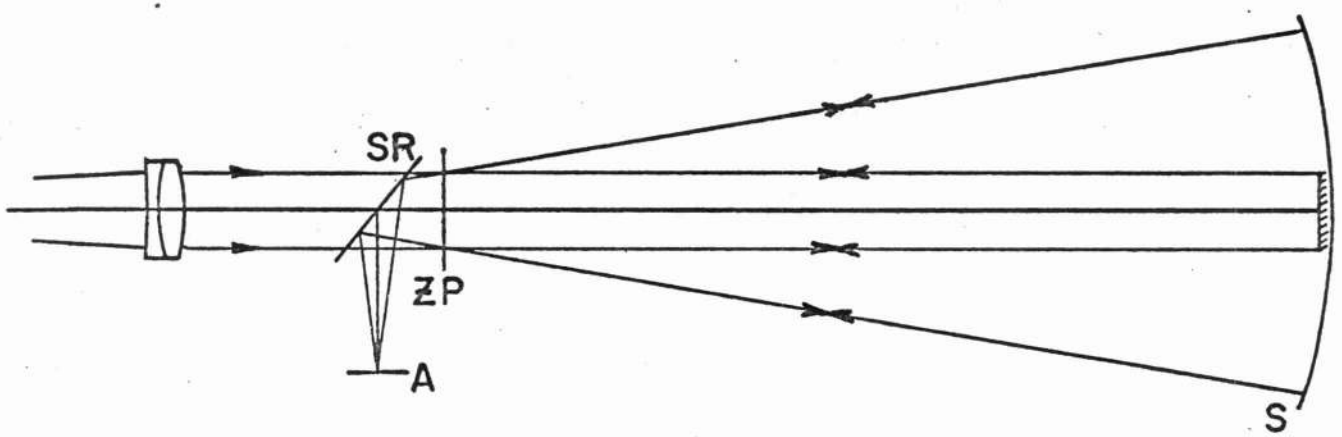

Fig. 10. Zone Plate Interferometer in mode 2. This version has a collimated reference beam and differs from the version shown in figure 8 which has a convergent reference beam.

tions as a corrected system and the test beam which it generates is not aberrated. The second and third modes now do not have an inverted wavefront, a further advantage. Moreover, most large astronomical primary mirrors have a hole through their center, and for common-path interferometer tests a separate mirror is required to reflect the reference beam. For a zone plate aperture of one centimeter, the plane mirror need only have the same aperture, and could be mounted on a simple fixture within the mirror hole, if necessary so that the plane mirror is tangent at its center to the test surface. It is not difficult to produce a plane mirror accurate to $\lambda/100$ over one centimeter, so that an accurate reference beam is assured.

2.2.5 Additional configurations

There is yet another configuration which should be mentioned, which although somewhat trivial, conceivably could be useful for some specific applications. Referring to Fig. 11, collimated light is incident on a zone plate, the first order principal focal length of which is equal to that of the concave mirror under test. The convergent first order beam in this case is the reference beam while the divergent first order beam is a test beam. The conjugate relationship between the real and virtual foci of the zone plate fulfills the required condition that when the reference beam is focused on the center of the mirror, the test beam has a virtual focus coincident with the center of cur-

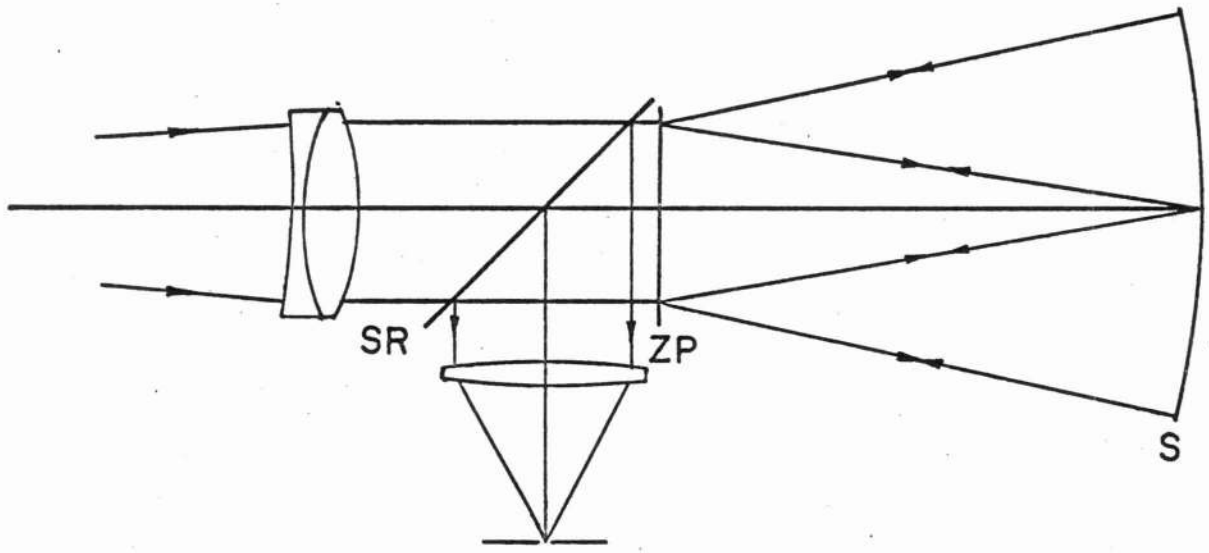

Fig. 11. Zone Plate Interferometer configuration in which the primary focal length of the zone plate equals that of the concave surface under test.

vature of the mirror. The interfering wavefronts form a collimated beam.

For completeness, it should be pointed out that multiple diffraction orders give rise to multiple configurations. For example, the interferometer can be set up using (2,0) and (0,2) beams, or (3,0) and (0,3) beams, and so on. In fact, if we allow test beams which have a non-zero order in the return path, the total possible combinations can be specified in the following manner:

	test beam	reference beam	
mode 1	$(\sum_i a_i, \sum_j a_j)$	$(0, a_i + a_j)$	$i=\pm1,\pm2,\text{--}$ $j=0,\pm1,\pm2,\text{--}$
mode 2	$(\sum_i a_i, \sum_j a_j)$	$(0, \lvert a_i\rvert + \lvert a_j\rvert)$	$i=-1,-2,\text{--}$ $j=0,+1,+2,\text{--}$
mode 3	$(\sum_i a_i, \sum_j a_j)$	$(0, -\lvert a_i\rvert - \lvert a_j\rvert)$	$i=+1,+2,\text{--}$ $j=0,-1,-2,\text{--}$

where for example a_{+1} represents a plus first order and a_{-1} equals $-a_{+1}$. Unless all these possibilities are recognized, one is confronted with a most perplexing array of interference patterns of unknown origin.

To be strictly rigorous, even the table above must be considered incomplete. Apart from some sign changes, the 'test beam' and 'reference beam' headings could be interchanged. This would then correspond to a configuration where a lens was used to generate a divergent test beam as a zero order on its first pass through the zone plate.

2.2.6 Summary

The configurations which have been proposed for the zone plate interferometer as set out in this chapter may be summarized in the following manner.

Three modes are distinguished according to the relative positions of the zone plate and the center of curvature, c, of the surface under test along the optical axis:

1. c is coincident with the center of the zone plate.
2. c is coincident with a virtual focus (first or higher orders) of the zone plate.
3. c is coincident with a real focus (first or higher orders) of the zone plate.

Different versions of these modes exist:

1. The direct (zero order) light is focused at the surface under test - a convergent beam.
2. The direct light is collimated.
3. The direct light is a divergent beam.

III. ZONE PLATES

3.1 Review of Zone Plate Theory

The classical (or 'Fresnel') zone plate has its origin in Fresnel's approach to the theory of diffraction. He used the artifice of considering a wavefront as being divided into elements or zones. The total wavefront behavior is then examined in terms of the contributions of the separate zones.

To illustrate this concept, consider the following construction, as represented in Fig. 12. PM_o defines an axis and the perpendicular line through M_o represents a plane in the three-dimensional case. The lines PM_j are incremented in their length in steps of $\lambda/2$, so that

$$PM_j = PM_{j-1} + \lambda/2$$
$$= PM_o + j(\lambda/2)$$

If the axis is rotated, these lines trace out circles of radii $M_1, M_2, M_3, \ldots$, which define the boundaries of the Fresnel zones (in the more general case these circles lie on a spherical surface rather than a plane). It follows that the radius M_j of the jth circle is given by,

$$M_j = \left[j\lambda z_o + (j\lambda/2)^2\right]^{\frac{1}{2}} \qquad (z_o = PM_o),$$

and the area of the (j-1, j) zone by,

$$\pi(M_j^2 - M_{j-1}^2) = \pi\left[\lambda z_o + (2j-1)(\lambda/2)^2\right].$$

The second term on the right hand side of both these equations is negligible except for large values of j.

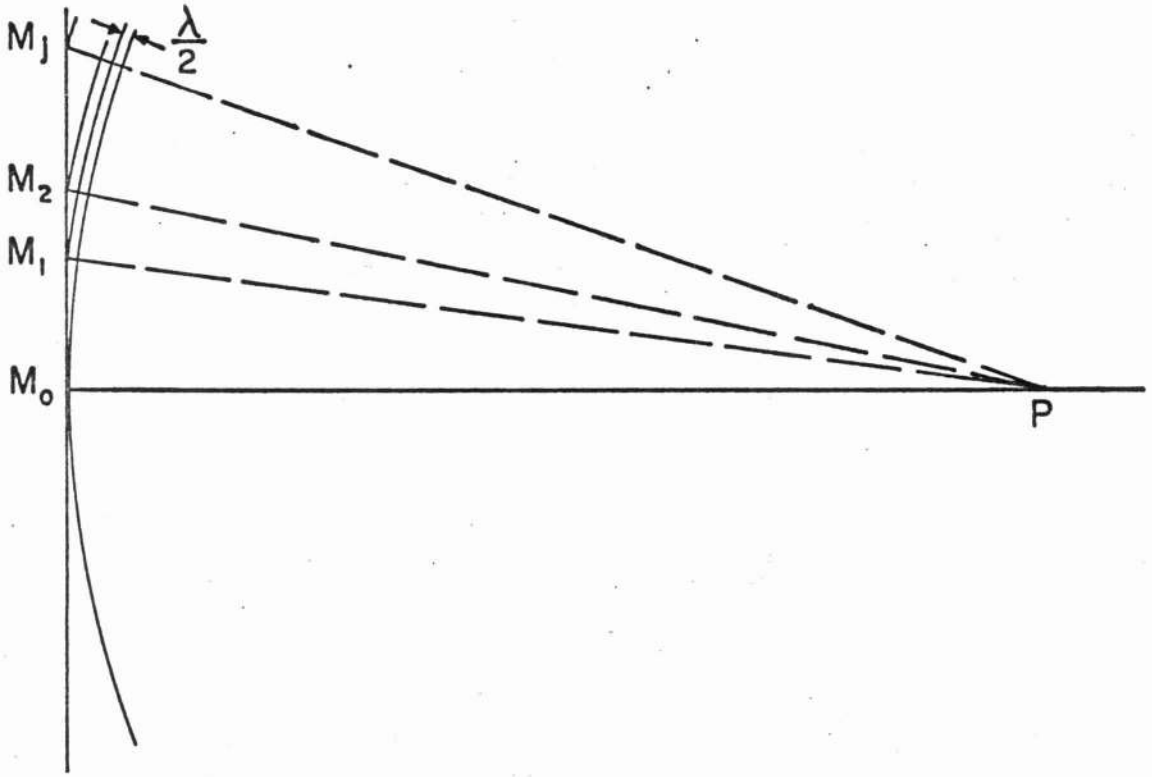

Fig. 12. Fresnel Zone Construction.

For these zones, the mean of the paths PM_j, PM_{j+1} (which define the (M_j, M_{j+1}) zone), differs by $\lambda/2$ from adjacent zones. A zone plate is formed when alternate zones are non-transmitting. Where a plane wave is incident on such a zone plate, the transmitted components are all in phase at the point P, which is then in effect a focal point of the zone plate. Rayleigh[9] suggested a modified form of zone plate - a phase zone plate - in which all zones are transmitting, the path through the zone plate itself differing by $\lambda/2$ between adjacent zones. All components then arrive in phase at a point such as P, with a fourfold increase in intensity.

Some authors make a distinction in name between the type of zone plate ('Fresnel') described above in which the amplitude transmittance across the zones is a rectangular function, and those which are characterized by other functions, for example a sinusoid ('Gabor'). Other names such as 'Soret', 'Binary', and 'Generalized', are also used. Such terminology is not followed here.

Consider a zone plate of diameter 2d with an amplitude transmittance

$$t(r) = 1/2(1 + \cos ar^2)$$, where a is a parameter characteristic of the plate, and r is a radial coordinate in the plane of the zone plate, with the origin at the center of the plate. We wish to find the form of the diffraction pattern characteristic of such a plate for a normally

incident, monochromatic, unit-amplitude plane wave, but limit this consideration to the axis of the plate, here the z-axis. In this case, using polar coordinates, the amplitude distribution U(0,z) for Fresnel diffraction reduces to,

$$U(0,z) = \frac{\exp(ikz)}{i\lambda z}\, 2\pi \int_0^d t(r).r.\exp\left(\frac{ikr^2}{(2z)}\right) dr \quad .$$

Let $u = r^2$, then

$$U(0,z) = \frac{\exp(ikz)}{2i\lambda z}\, \pi \left\{ \int_0^{d^2} \exp(iku/2z)du + \tfrac{1}{2}\int_0^{d^2} \exp\left[iu(k+2za)/2z\right] du + \tfrac{1}{2}\int_0^{d^2} \exp\left[iu(k-2za)/2z\right] du \right\}$$

The first integral represents just a plane wave, that is the non-diffracted light, while the second and third integrals represent spherical waves, with radii of curvatures of $z=-k/2a$ and $z=k/2a$ respectively. Such a zone plate therefore has only two 'foci', symmetrically positioned either side of the plate.

In the more general case however, multiple foci occur. The amplitude transmittance for a rectangular distribution across the zones is conveniently expressed in the form

$$t(r) = U.(\cos ar^2) \qquad U(x) = \begin{cases} 1 & x \geqslant 0 \\ 0 & x < 0, \end{cases}$$

while the equivalent phase plate has a transmittance

$$t(r) = \operatorname{sgn}(\cos ar^2) \qquad \operatorname{sgn} x = \begin{cases} 1 & x > 0 \\ -1 & x < 0 \end{cases} .$$

The 'square wave' which this function describes may be represented in turn by the Fourier series

$$f(x) = \sum_{n=-\infty}^{\infty} \frac{\sin(\pi n/2)}{\pi n} \exp(i2\pi nx/X)$$

where X is the period. (This is obtained from Poisson's sum formula which states that for any arbitrary function h(x) with transform H(f),

$$\sum_{n=-\infty}^{\infty} h(x + nX) = \frac{1}{X} \sum_{n=-\infty}^{\infty} H(nf).\exp(infx) \qquad f=\frac{2\pi}{X} \quad)$$

If this sum f(x) is taken as the amplitude transmittance t(r) for the above phase zone plate, we have $X = (n)^{\frac{1}{2}} - (n-2)^{\frac{1}{2}}$, and a sum of integrals for the amplitude distribution U(0,z) is obtained. It is found that alternate integrals are zero and the remainder represent spherical waves, the radii of curvature of which decrease as the reciprocal of successive odd integers. That is, the focal lengths of these plates are specified by the relation

$$f_i = \frac{f_o}{(2i+1)} \qquad i = 0, \pm 1, \pm 2, \ldots$$

It has been shown[10] that a zone plate which has some transmittance function intermediate between the two extreme cases cited above can have foci given by,

$$f_i = \frac{f_o}{i} \qquad i = \pm 1, \pm 2, \ldots$$

3.2 Construction of Zone Plates

When a spherical and a plane wave interfere, the resultant interference pattern has a distribution of fringes which characterizes a Fresnel zone system. Consequently, when such a pattern is recorded photographically, the

developed image has the properties of a zone plate. Only with special processing is the amplitude transmittance likely to approach a rectangular function, since the fringes have a cosine-squared intensity distribution and the image has a significant longitudinal dimension within the emulsion. In any case, the photographic process is intrinsically non-linear and if the silver image is converted by bleaching to a relief image (described below), further non-linearities are produced even to an extent where some compensation may be required. Nevertheless, this modified form of Fresnel zone plate has the basic properties of the classical description, the difference in terms of energy distribution within the various orders being an advantage for this application.

In the work reported here, zone plates were constructed using the optical system represented in Fig. 13. The beam from a He-Ne laser LA is divided into two components by means of a variable-transmittance beam-splitter BS[11]. The transmitted component is expanded by the objective O_1 and lens L to form a collimated beam, in this case about 4cm diameter. The other component follows the separate path shown, and without the microscope objective O_2 in the system, is aligned to be coaxial (after the last reflection) with the transmitted beam. The objective O_2 and a pinhole are then inserted to give a divergent, spherical wavefront, forming with the collimated beam the desired interference

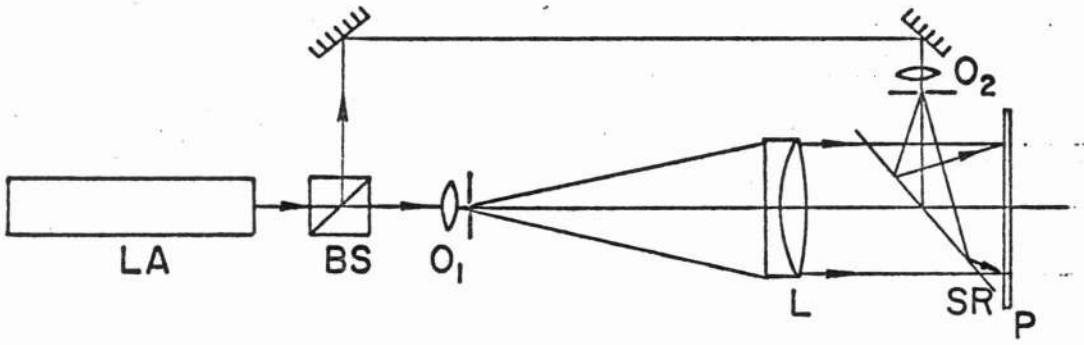

Fig. 13. Optical system used to construct zone plates. LA, laser; BS, variable transmittance/reflectance beam-splitter; O_1, O_2, microscope objectives; L, collimating lens; SR, semi-reflector; P, photographic plate.

pattern. As in most holographic work a system free from vibration and thermal fluctuations in the air path is necessary. To generate an accurately spherical wavefront, a 0.85 numerical aperture microscope objective was selected with a wavefront error $<0.1\lambda$. High contrast fringes were obtained by operating the laser in a single mode and by adjusting the variable transmittance beam-splitter to equalize irradiances in the recording plane. The interference patterns were recorded on 1mm and 6mm thick, 649F photographic plates, with the emulsion side facing the incident light, care being taken to mount the plates normal to the optical axis, and without distortion. Reflection from the back surface during exposure was eliminated by coating it with a toluene-based ink. This system allows zone plates to be constructed down to f/1, where the primary or first order focal length is taken as the principal focal length; for the f/1 zone plates used, about 4cm.

3.2.1 Characteristics of the image

The central region of a zone plate made by this method using standard development procedures is shown in Fig. 14. The magnification is 50X. A superimposed interference system is also evident which consists of finely spaced, straight fringes. They originate in light reflected from both surfaces of the semi-reflector, but in no way apparently impair the performance of the interferometer. For an optimum density of about 0.5, zone plates of this

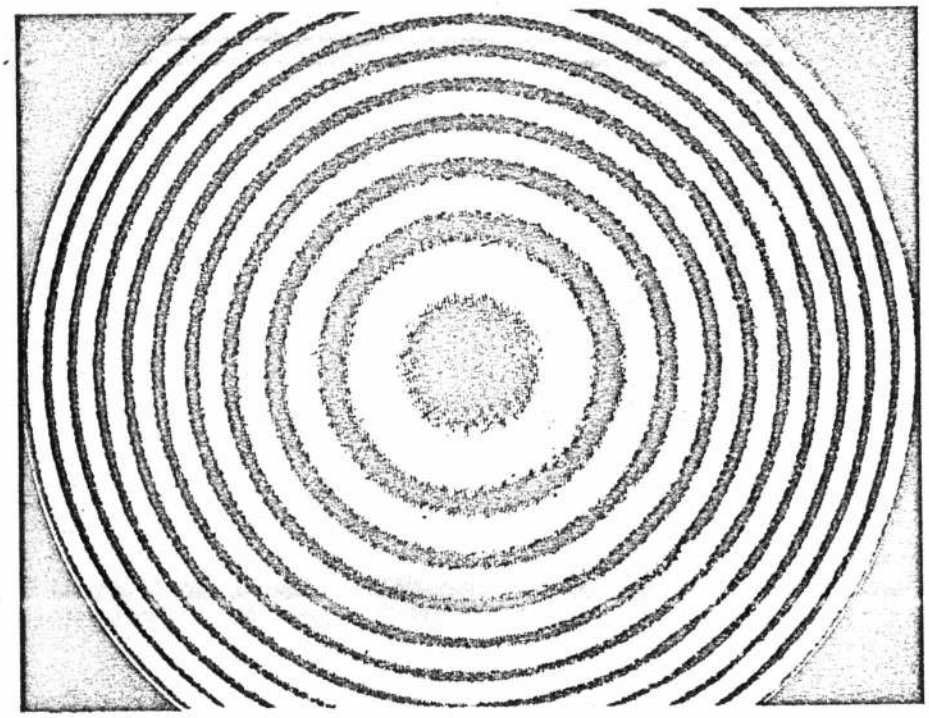

Fig. 14. Central region of a zone plate; magnification 50x.

amplitude type have a transmission in the first order of only a few percent[12]. Consequently, the interferometer will be comparatively inefficient, although even a low power laser source is more than adequate for visual use.

It has been pointed out[13] that the zones of a zone plate made in this way are not confined to one plane since the fringes are recorded in depth through the emulsion (about 15μ for 649F plates). The Bragg-like reflection that can occur at the three-dimensional silver image results in some enhancement of the light diffracted into certain orders, particularly for rays diffracted through large angles. This property is favorable in mode 2 of the interferometer for both first order diffracted wavefronts when the emulsion side of the zone plate faces the source.

3.2.2 Bleaching of zone plates

The efficiency increases when the zone plates are bleached to form pure or partial phase gratings. Several bleaching processes were tried. The method given by Altman[14] was found to be the most satisfactory for this application. The exposed plate is bleached after development and before fixing which leaves a relief image alone in place of the silver image. The central part of a zone plate bleached by this method is shown in Fig. 15, a microphotograph taken with vertical illumination at 50X magnification. The striking three-dimensional form of the surface is clearly evident. The contour of course varies with exposure. It is remarkable

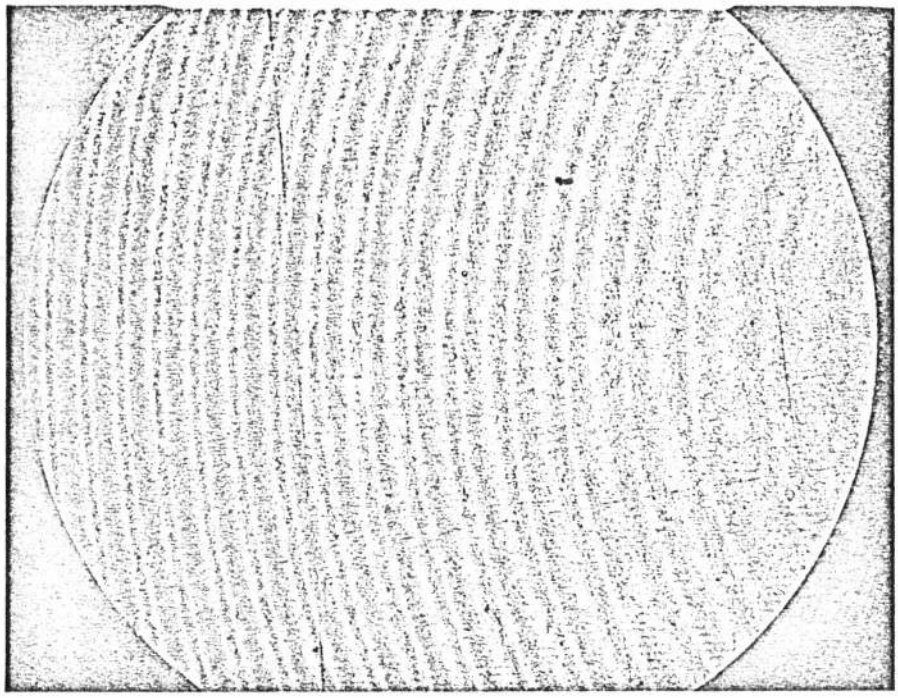

Fig. 15. Central region of a bleached zone plate; magnification 50X.

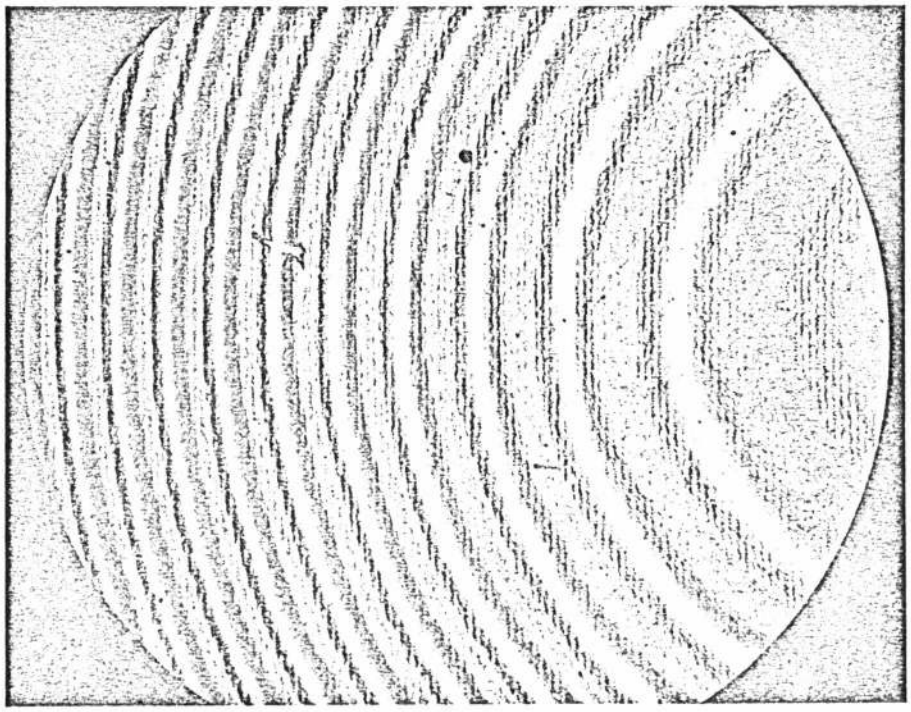

Fig. 16. Central region of a partly bleached zone plate; magnification 50X.

that even fine details in the original image are substantially preserved. For example, note the fine, straight system of lines - a fringe system - superimposed on the circular pattern, similar to the feature pointed out above in Fig. 14.

Alternatively, the photographic plate may be processed in the normal manner and then bleached to a point where the developed image has barely disappeared. The center of a plate prepared in this way is shown in Fig. 16. An enhanced relief image is evident as before, but differs from the previous case in that a residual image can also be seen when the zone plate is examined in transmitted light. These plates have a higher diffraction efficiency and are more suitable, for reasons pointed out below, to cases where the primary focus is less than a few centimeters.

3.2.3 Compensation to obtain uniform amplitude wavefronts

It is known that even normal processing leaves the emulsion surface higher in regions which contain a silver image than in adjacent clear regions[15]. The amount of local elevation or relief is proportional to the amount of silver in the image, but varies with spatial frequency. In the case of bleached plates, this variation of relief with spatial frequency becomes increasingly non-linear as the spatial frequency decreases. Evidence of this effect is found in the intensity distribution of collimated light reflected from the surface of an amplitude zone plate. For zone plates

with a primary focus of about 10cm, there is an annular region of mean diameter about 1cm where the reflected light falls close to zero. The diameter of this region increases with exposure to an extent where further minima may occur closer to the center, and shrinks in diameter as the zone plate focus decreases. For a primary focus of 4cm, a diameter of 4 or 5mm is typical. The effect was not observed for 20cm plates. The lowered reflectance is attributed to a phase difference of π between the light diffracted from adjacent 'high' and 'low' zones. We note in passing that this phenomenon suggests a unique form of anti-reflection coating, conceivably of use in some special application.

It turns out that after bleaching the region previously of low reflectance becomes one of low transmittance, evident in all orders. This is again attributed to a phase difference of $n\pi$ (where n is unity or a higher odd integer) over some critical band of spatial frequencies. Note that even if the relief in the emulsion due to the bleaching process were independent of spatial frequency and quite linear with respect to the developed density of the silver image, the constant of proportionality critically determines the phase difference and therefore the efficiency of the zone plate. The typical intensity variation of a zero order beam transmitted by a bleached zone plate is indicated in Fig. 17.

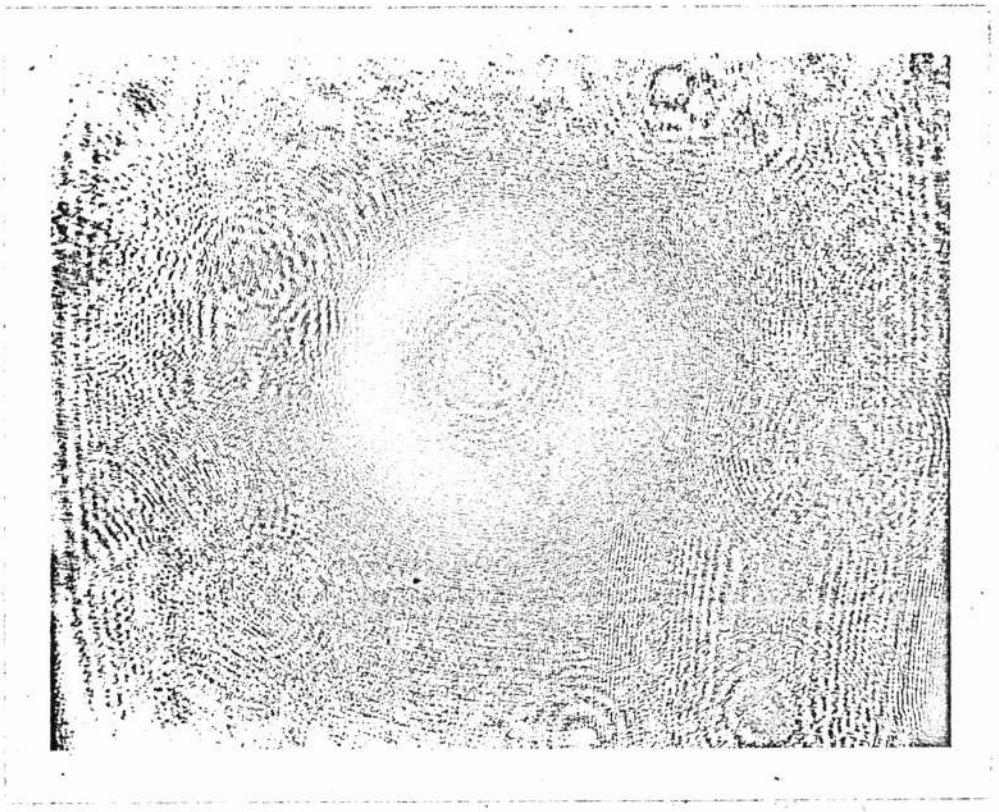

Fig. 17. A photographic recording of the zero order beam (cross-section) of a bleached zone plate, showing the typical variation of intensity.

The corresponding amplitude distribution will be contained in the test and reference wavefronts and the interferogram will thus have a similar non-uniformity. If air is replaced by a medium of higher refractive index bounding the diffracting surface, the non-uniformity diminishes, as the index increases, until it merges with the rest of the field. Beyond this, a reversal (overcompensation) takes place such that the mean irradiance at the center of the interference pattern becomes greater than that at the edge. It is fortuitous that the optimum refractive index usually lies within the range of stable oils available as refractive index standards. A wavefront having an approximately uniform amplitude may then be obtained by the use of an appropriate index oil as a film between the gelatin surface and a plane cover glass. As an example, for pure phase zone plates with a primary focal length of 10cm, the ideal index has been found to be in the range 1.35 to 1.45. The amplitude correction is made with a sacrifice in diffraction efficiency; nevertheless, the efficiency remains substantially greater than for amplitude zone plates.

It has been found that complete compensation for phase zone plates having a primary focal length less than about 5cm is generally not possible, and the best choice of oil index is a compromise which leaves a dark central spot in the interferogram. If, however, the zone plates are bleached after normal processing to leave a relief and amplitude image,

diffraction efficiency is higher compared with pure phase gratings, and oil of about 1.55 refractive index again produces a constant amplitude. A second cover glass, with matching index oil, may be added with advantage at the rear (glass) surface of the zone plate, in cases where this surface is not plane.

3.3 Testing of Zone Plates

Moiré fringes provide a simple measurement of the overall accuracy of a zone plate. It has been shown[16, 17], using an indicial representation, that the moiré pattern of two identical zone plates consists of parallel, equi-spaced straight lines. The spacing is inversely proportional to the separation of the centers of the zone plates. Oster[17] points out that for a separation 2s of the centers greater than $2\sqrt{\lambda b}$, where b is the primary focal length, a moiré zone system results. This is illustrated in figure 4 of reference 17. Curiously, the straight line moiré pattern which is to be expected is not obvious in this figure and is not mentioned in the text. However, it can be seen clearly when the figure is viewed at glancing incidence. In fact this moiré pattern is the dominant one in all cases where the scale of the zone plates is such that only the first few central zones can be distinguished with the unaided eye. It should be mentioned that the above discussion and that to follow is based on the approximate description of a Fresnel zone plate where the

radii of the circles defining the zone systems are proportional to the square roots of the natural numbers.

Consider the case where the zone plates are not identical. The equations of the two zone systems, with the centers separated by a distance 2s, may be represented as,

$$(x - s)^2 + y^2 = h$$

$$(x + s)^2 + y^2 = ak$$

where h and k are the indexing parameters, each a subset of real integers, and $a^{\frac{1}{2}}$ is the magnification factor between the two systems. The moiré pattern is then given by the equation:

$$x^2 + y^2 - 2xs\left(\frac{a + 1}{a - 1}\right) + s^2 = \left(\frac{a}{a - 1}\right) p \quad , \qquad a \neq 1$$

where $h - k = p$ is the indicial equation. This is a zone system of circles.

An example is given in Fig. 18, a moiré pattern of two phase zone plates which differ slightly in focal length. The apparent discontinuities of the moiré fringes in this photograph are simply the result of some non-uniform illumination.

The value of this check is further illustrated in Fig. 19, where an error in one of the zone plates stands out sharply. The two plates are identical, except in one the central region differs in focal length from the surrounding annular region.

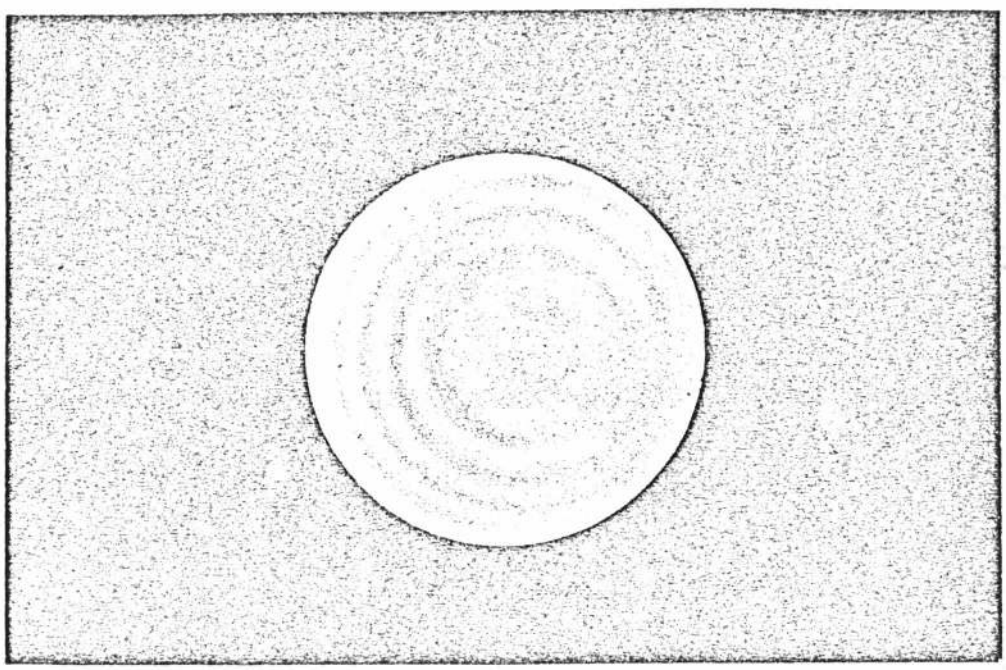

Fig. 18. Moiré pattern of two phase zone plates differing slightly in focal length.

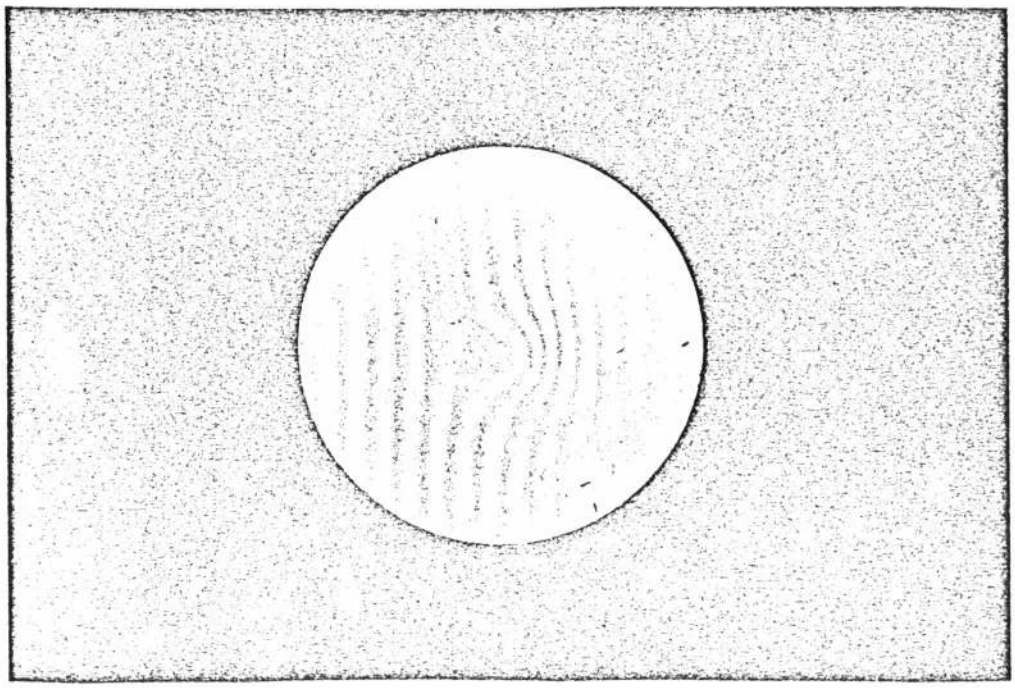

Fig. 19. Moiré pattern of two phase zone plates which have the same focal length, apart from the central region of one plate which differs in focal length from the surrounding annular region.

IV. CONSTRUCTION OF A ZONE PLATE INTERFEROMETER

The optical system described in Chapter 3 for the construction of zone plates can be adapted with only slight modifications to form a zone plate interferometer. Such an interferometer has been constructed, and is represented schematically in Fig. 20.

4.1 Components

4.1.1 Laser source

For most experiments, a He-Ne laser with a nominal beam power of 25mW was used. In practice, this power level would diminish following servicing, typically to a few milliwatts after several days, due mainly to the accumulation of dust particles on the Brewster angle windows, the reflectors and an intra-cavity prism. It was found convenient each time the laser was used to remove the end dust covers and clean the optical surfaces with a cotton pad saturated with acetone, a simple operation which resulted usually in an increase to about 15mW or more. Even though an output of less than one milliwatt is more than adequate for an interferometer source, a higher power is far more convenient. This allows the beams to be traced throughout the system(using for example a white sheet of cardboard) - a considerable advantage in determining the overall behavior of each system. The first few orders of the zone plate can usually be observed, and

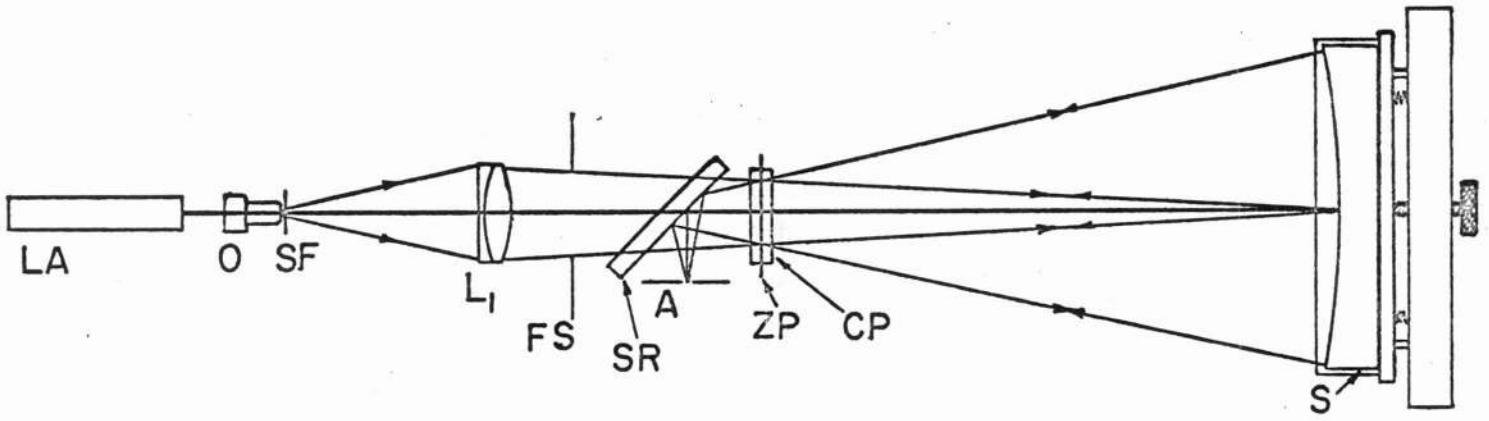

Fig. 20. Schematic diagram of the zone plate interferometer. LA, laser; O, microscope objective; SF, spatial filter; L_1, lens used to form an image of the source at the surface under test; FS, field stop; SR, semi-reflector; ZP, zone plate; CP, glass cover plates; S, surface under test; A, aperture.

the 'projected' interference patterns seen clearly in this way. Of value also is the ease of alignment of the zone plate and other components as determined by the position of reflected images, and the detection of relatively faint amounts of stray light.

The laser was mounted directly on the optical bench and an adjustable double mirror system employed to elevate the optical axis, and thus increase the upper limit for the diameter of test components. The beam was expanded to fill the 5cm aperture of an f/4 lens, in fact a collimating lens shown as L_1 in Fig. 20, by means of a microscope objective of numerical aperture 0.65. The lens and microscope objective together establish the optical axis of the interferometer.* The lens L_1 was mounted on an accurate slide so that its position could be adjusted along the axis to form an image of the source at the test surface. But such a system is uncorrected, since the lens is operating at finite conjugates. It is shown below that the resultant wavefront error has a negligible effect upon the performance of the interferometer.

4.1.2 Zone plate mounting

The zone plate was mounted in a simple vertical holder, and clamped with its center in the horizontal plane

*While the laser beam establishes an optical axis, once the microscope objective is inserted in the beam, only a point is defined - the focus of the objective.

containing the optical axis. The base of the holder could then be moved in a horizontal plane such that the optical axis would pass normally through the center of the zone plate. Even when the holder was left unclamped to the optical bench, no vibration effects were observed in the interference pattern, an advantage of the common-path design.

4.1.3 Test mirror mounting

Several concave mirrors of different diameters have been tested with the interferometer and for this purpose an aluminum holder was constructed capable of supporting mirrors ranging from two inches to seven inches in diameter. To avoid distortion of its surface, the mirror under test rests on its edge in a vee mount which is attached with bolts which pass through slotted holes to a backing plate. The vee mount can thus be moved in a vertical direction to position the center of each mirror on axis. A light adjustable clip retains the mirror against the backing plate. The backing plate can be tilted about a horizontal axis, but for simplicity of construction, no corresponding controlled adjustment about a vertical axis was incorporated. The holder can be locked to the metal optical bench by its three magnetic bases, although experience has shown that due to its rugged construction this precaution is not normally necessary.

4.1.4 Beam-splitter

A semi- or partial reflector is required to observe the interference pattern. Its function is to reflect light and since this occurs external to the interferometer proper, the reflecting surface need only be plane to an accuracy (1 wavelength/cm) such that no significant image distortion occurs. In the experimental work reported here, a plane-parallel plate of glass about 1cm thick was employed for this purpose, with a reflective coating on the surface nearer the zone plate. It was positioned not at 45° to the axis of the interferometer, but closer to the Brewster angle, to reduce the light reflected from the uncoated back surface. For maximum efficiency the reflectance r should be 0.5, but the transmittance of the interferometer is a slowly varying function of r, the specific value of which is therefore not critical. The optical quality of this component is mainly of importance only in its disturbance to the transmitted wavefront incident on the zone plate. For an object not at infinity, primary and secondary astigmatism, coma, and spherical aberration are introduced, as well as lateral and longitudinal image shifts. However, all aberrations which have axial symmetry will self-cancel in this two-beam system, and therefore will not be recorded in the interference pattern.

For a ray incident on a reflector of thickness d at an angle θ, components reflected from both surfaces are laterally separated by an amount

$$s = 2d \cos\theta \tan\theta' \quad ,$$

where θ' is the angle of refraction. When the angle of incidence $\theta = 45^{\circ}$, and the refractive index of the substrate is 1.5, the separation s is approximately 0.7d. A reflector for which the 'back-surface' reflection is not negligible must have a thickness d such that either the source images are clearly separated, or they are superimposed with at most only a small percentage error. The latter condition is fulfilled with a pellicle film. Otherwise, two overlapping interference patterns will occur.

At first sight it might appear that a pellicle type partial reflector would in principle be preferable to a much thicker glass plate. The thickness of pellicle films is at most only a few wavelengths and hence aberrations are negligible apart from those due to irregular variations in thickness. However, while pellicles are available which have surfaces parallel to a few wavelengths, any residual inclination between the surfaces can give rise to an interference pattern which modulates the amplitudes of the reflected beams, and strongly so for such thin films unless the surfaces are appropriately coated. Also it is likely that the reflecting surface of a pellicle will not be plane to the same accuracy as its surfaces are parallel. The former property is the most important.

4.1.5 Aperture

As discussed in Chapter 2, many different wavefronts are generated by the interferometer. The two desired interfering components can be conveniently separated from all other wavefronts by placing a small aperture at the appropriate image of the source. The diameter of the aperture can be less than 0.5mm without any vignetting of the interference field taking place, a measure of the accuracy of the refraction-like process in these zone plates. Since all other wavefronts have different cone angles, a negligible amount of stray light passes through the aperture stop. The zero-zero order light can normally be seen as a bright spot in the center of the field only when the interference pattern has a destructive interference fringe passing through the center of the field and only in a plane close to the aperture. A three-dimensional micrometer table on which the aperture was mounted was incorporated in the interferometer. This device allowed the aperture to be adjusted easily and quickly to be co-planar with and centered on the image. A disadvantage of such a small aperture/stop to exclude as much stray light as possible is that the depth of focus for a camera lens focused on the aperture of the system under test becomes excessively large, and a sharp image cannot be obtained.

A field stop in the form of an iris diaphragm was also incorporated in the interferometer between the lens L_1 and the partial reflector.

4.1.6 Compensating oils

It has been mentioned in Chapter 3 that the performance of a zone plate of either the pure or partial phase types is improved when an oil (of appropriate refractive index) and cover glass are added to its surface. The compensating oils used were from the range produced commercially as refractive index standards. They are specially prepared to be free from water and have no apparent effect on the photographic emulsion, even over long periods, and although mostly mixtures, the index varies little with evaporation. Below a refractive index of about 1.38, the oil viscosity is low and does not remain as a continuous film for more than about one day, but drains away or evaporates unless enclosed in a special cell. In the range between about 1.45 to 1.55, the oils are more viscous and stable, and remain as continuous films almost indefinitely even without using a cell. The area of the cover glasses used was of the order of ten square centimeters.

4.2 Interferometer Adjustments

4.2.1 Alignment of components

An important feature of this interferometer is the ease with which it may be 'set up' for testing a telescope lens or concave mirror, and the ease with which the interference pattern is then obtained.

Initial alignment of the interferometer is most easily accomplished, as with similar optical systems, by using the laser beam unexpanded to define an optical axis and setting the zone plate and other components accurately to this reference.

Referring again to Fig. 20, the aperture of the mirror M is centered with respect to the optical axis with its center of curvature close to the appropriate position for the selected mode. The lens L_1 is then positioned to focus the source approximately at the test surface, a condition which can be checked easily by placing a piece of paper at the center of the mirror surface. The reflected light (reference beam), passing through the zone plate, then establishes a set of conjugate focal positions. For moderate to high f-number systems, the first order image can be identified uniquely since its position will differ by only a small amount from the principal first order focus of the zone plate, and this establishes in turn an approximate position for the aperture A. The mirror is then moved along the optical axis so that the test beam is focused in the same plane as the reference beam, while slightly correcting the position of the lens L_1 if necessary. Next, by further adjustment of the mirror, the images are brought to coincidence, and the aperture A centered with respect to them. At this stage it should be possible to observe an interference pattern beyond the aperture. If this is a centered system

of circular fringes, the center of curvature of the mirror lies on the optical axis. For a spherical mirror the number of fringes in the field may be reduced to zero by either increasing or decreasing the separation between the mirror and zone plate, depending on the setting. At this position, straight, equally-spaced fringes are introduced across the field as the mirror is translated laterally or tilted. Departures from this pattern are a direct measure of variations in the mirror surface from a spherical contour.

Even if the zone plate is not accurately centered or is tilted slightly with respect to the axis, the two wavefronts of interest, though now distorted, still interfere. Asymmetry of the interference pattern due to such misalignment is easily recognized where the mirror under test is spherical to within a small fraction of a wavelength. This is in contrast to the scatter-plate interferometer which must be aligned very precisely before any interference can be achieved.

4.2.2 Differential image movement

In most applications of double-focus interferometers the reference and test beams are both reflected at the surface under test, for example a concave mirror. For a small mirror tilt $\delta\theta$, the reflected beams are both rotated through the angle $2\delta\theta$, and hence there is no differential movement between the wavefronts. Therefore it might appear at first sight that since the path difference remains unchanged, the interference fringe pattern is independent of small mirror

tilts. That this is not so may be seen by considering the second mode of the zone plate interferometer, a generally representative example. It is illustrated in Fig. 21. The reflected beams are indicated by broken lines, the reference beam initially a divergent wavefront and the test beam a convergent wavefront. Now the center of curvature of the reference wavefront is fixed in space, that is on the optical axis at the mirror surface. Therefore, even though the reference wavefront shifts laterally with mirror tilt, it is always tangent to the zone plate at its center, and the first order image thus remains stationary, independent of mirror tilt. The intensity in this image diminishes with angle of tilt if the wavefront does not lie entirely within the zone plate aperture. For the reflected test wavefront, the situation is quite different. The position of its center of curvature is remote from the mirror and consequently is a function of the angle of tilt. In this particular example the test wavefront in its second pass through the zone plate is a zero order, and the position of the source image which it forms is thus determined by the law of reflection. It follows that to obtain an interference pattern, the mirror surface must be adjusted to move the test beam source image to be coincident with the stationary reference beam source image.

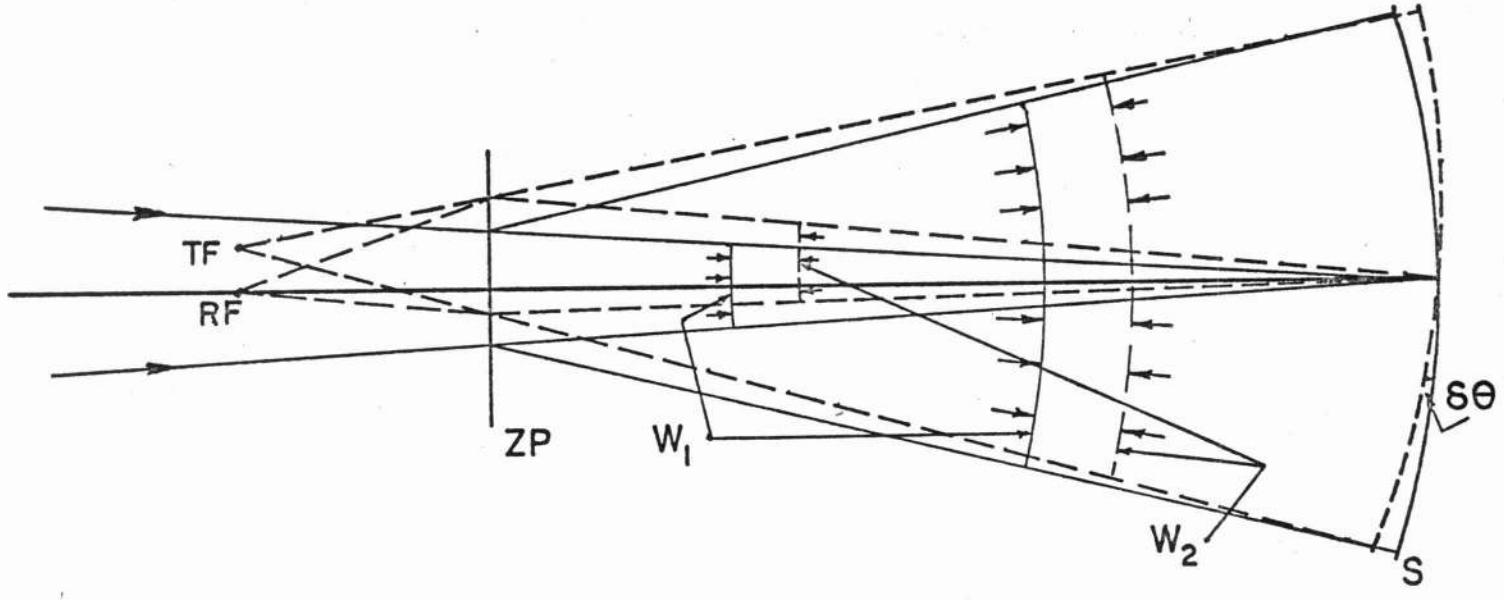

Fig. 21. Relationship of mirror tilt to reference and test beam foci. ZP, zone plate; S, surface under test; W_1, incident wavefronts; W_2, reflected wavefronts; TS, test beam focus; RF, reference beam focus.

4.3 Holography

4.3.1 Multiple sources

It has been pointed out in Chapter 2 that a complex array of interference patterns is generated by a zone plate interferometer. These patterns arise from the many possible combinations of the multiple diffraction orders of a zone plate. In practice the situation can be even more complex, perhaps best understood from the point of view of holography. A zone plate can be considered as an elementary hologram, which 'reconstructs' real and virtual images of the source in the first and higher orders when appropriately illuminated. The method already described for the manufacture of zone plates is that of recording an interference pattern photographically. The two wavefronts which are required to produce this interference pattern can be considered as the two components of a hologram - the wavefront which is to be recorded and the reference wavefront. The particular role of the spherical and plane wavefronts from this viewpoint is of course arbitrary. But in any optical system such as that used to prepare the zone plates, it must be expected that secondary sources will exist such as 'ghost' images and multiple reflections, and these will also be reconstructed by the hologram zone plate. An example is where the partial reflector has significant internal reflections. For a ray incident at an angle θ, multiple components are transmitted

and reflected as parallel bundles spaced laterally by amounts $2d \sin\theta \tan\theta'$ and $2d \cos\theta \tan\theta'$ respectively, where θ' is the angle of refraction. It follows that a spherical wave, multiply reflected, gives rise to multiple virtual sources laterally displaced, while a plane wave gives a series of laterally displaced plane waves, but the virtual sources in this case have no lateral separation unless the partial reflector surfaces are not parallel. These are coherent sources and the wavefronts mutually interfere.

4.3.2 Reconstruction of sources

An examination of the zone plates under a microscope reveals not only an image of the main zone system of fringes with a very fine, apparently random, superimposed modulation, but a number of subsidiary zone systems symmetrically positioned either side of the main system, as well as a closely spaced system of straight, parallel fringes.

The subsidiary zone systems obviously arise from the multiply reflected spherical waves, and each reconstructs a displaced virtual source when the zone plate is illuminated in the interferometer. Instead of a single first order image therefore, it is usual to find a row of images, all higher 'orders' of the first order of the zone plate. (The level of irradiance in the 'zero'-first order image allows it to be easily distinguished from the secondary images.)

Since the partial reflector used in this work was parallel to within a few wavelengths, the system of straight

fringes is attributed to interference between the displaced spherical wavefronts. That the fringes are straight follows from the theorem which may be stated as,'the projection of the line of intersection of two overlapping spheres onto a plane parallel to that plane containing the centers of the spheres is a straight line'. The recorded fringes thus may be considered as a grating with a spatially varying period, which in turn gives rise to reconstructed wavefronts.

All the zone plates reveal a faint fringe-like pattern when observed in reflected light. The origin of this pattern proved to be two-beam transmission fringes of the air-spaced collimating lens, clearly evident as a reconstructed virtual image when the zone plate is illuminated with a coherent reconstruction wave. A number of other secondary sources within the recording system were identified, each giving rise to an interference pattern. Even so, despite the presence of all the extraneous wavefronts generated by the zone plates, there is no obvious detrimental effect on the performance of the interferometer.

4.4 Comparison with a Twyman-Green Interferometer

Beyond demonstrating the practicality of a new device such as the interferometer, it is important to consider its relative merit compared with other devices which can be used for the same purpose. A simple comparison has been made between the zone plate interferometer and a compact Twyman-

Green interferometer constructed at the Institute of Optics in 1966[3].

The Twyman-Green interferometer employed in this study is an unequal-path type designed for use only with a laser source. The interferometer is basically a compound prism, consisting of two prisms cemented over two surfaces which are inclined at an angle of 30° to the plane-parallel external surfaces. The second of these surfaces performs the function of a beam-splitter since that part of the incident light reflected from it constitutes the reference beam. One of the cemented surfaces has a partially reflective coating and allows the interference pattern to be observed through a side face. The prism operates in parallel light and has a maximum aperture of about one centimeter. For applications typical for common-path interferometers, the prism must be combined with a lens system to produce an accurate, divergent spherical wavefront.

What is involved in the construction of an optical system such as this compact Twyman-Green interferometer? Two prisms must be constructed from hgih quality optical glass, four of their surfaces polished plane to a moderately high accuracy, and one surface, the exit face, to an accuracy of $\lambda/20$ or better, since this produces the reference wavefront, and errors are only partially compensated by the test wavefront. The surfaces must also have high angular correction and one internal surface appropriately coated.

To reduce multiple reflections of the collimated light between the three external faces, high efficiency anti-reflection coatings are also desirable on these surfaces. Cementing of the prisms so that they are accurately aligned and with the cement film free from bubbles is normally a routine operation. The lens system must have a high degree of correction since any aberrations which it introduces will affect only the test beam, and doubly so since the beam passes twice through the lens. In support of this statement, experience with the interferometer has revealed that the lens must be very accurately aligned. Otherwise the interference fringes show a marked pattern characteristic of astigmatism. By contrast with the amount of labor involved in the construction of the Twyman-Green interferometer, the manufacture of a zone plate is far simpler. As an example of this, more than 50 zone plates were made during the development of the zone plate interferometer.

Nevertheless, the viewpoint may be taken that labor required for the construction of an interferometer is relatively unimportant compared with the quality of its performance.

4.4.1 Twyman-Green interferometer test

A concave mirror, spherical to less than one wavelength, was selected for test. The mirror aperture was 15cm with a radius of curvature of 75cm. For maximum visibility of the fringe pattern, the amplitudes of the interfering beams must be equal. The Twyman-Green interferometer has been designed

for tests of uncoated optical surfaces, and the exit face of the interferometer therefore has no reflective coating. Consequently, when the aluminized mirror was set up for test, fringes of very low contrast were obtained. In an attempt to balance the amplitudes of the two beams, a neutral density filter was inserted in the test arm in the collimated region to reduce the amplitude of this wavefront. Note that a plane-parallel plate, even if optically perfect, introduces some aberrations when placed in a non-collimated beam. Also, optimum fringe visibility is possible for a multi-mode laser source of cavity length l only when the interferometer path difference has the value $2ml$ $(m=0,1,2,...)$.

A characteristic of unequal-path interferometers is their sensitivity to mechanical vibration and thermal fluctuations in the air path of the test arm, and a measurable distortion of the interference pattern due to these causes may be registered in the interferogram. The two interferometers were set up on a large metal optical bench supported on anti-vibration pads. These were not very efficient and the interference pattern produced by the Twyman-Green interferometer was found to move almost continuously, both from the effects of vibration and index variations in the air path.

4.4.1.1 Recording the interference pattern

To photograph the T-G interference pattern, a 35mm reflex camera was employed and more than thirty exposures

taken using FP3 film. Exposure times were varied from 1/30 sec to 1/250 sec and an attempt was made to expose the film during the occasional intervals of a second or so when the fringe pattern appeared to be stable. Nevertheless, the developed film revealed some variation in fringe contour between the different exposures amounting at most to about $\lambda/10$. The most commonly occurring pattern was taken as being closest to that free from transient effects, a reasonable assumption since the disturbances tend to be quite random. One of these interferograms is shown in Fig. 22. Associated with the primary interference pattern is some fine structure attributed to interference between the reflected components within the prism.

4.4.2 Zone plate interferometer test

The mirror was left in position in its mount to preserve orientation and then tested using the zone plate interferometer set in the second mode. The interferogram obtained by this means is shown in Fig. 23, in which the mirror was carefully adjusted to give close to the same fringe distribution as in the previous figure, thus allowing an accurate comparison.

In a comparative test such as this, it is important to ensure that the component under test is in a state of thermal equilibrium, since the thermal conductivity of glass is comparatively low. For this reason, interferograms were recorded only after the room temperature had remained constant to less than one celsius degree for several hours.

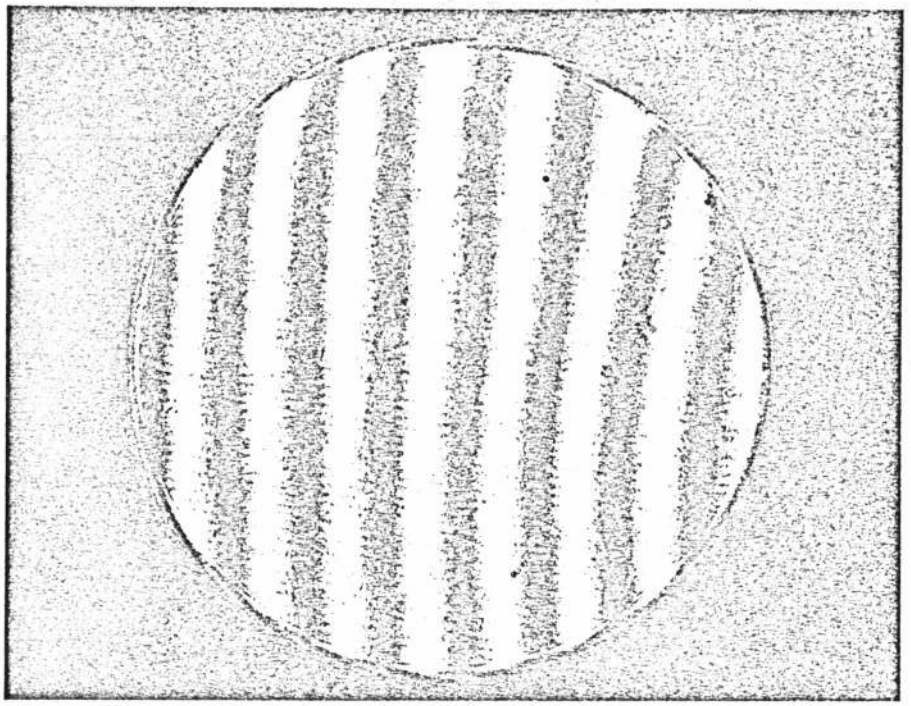

Fig. 22. Interferogram of an f/2.5 concave mirror obtained using a compact Twyman-Green interferometer.

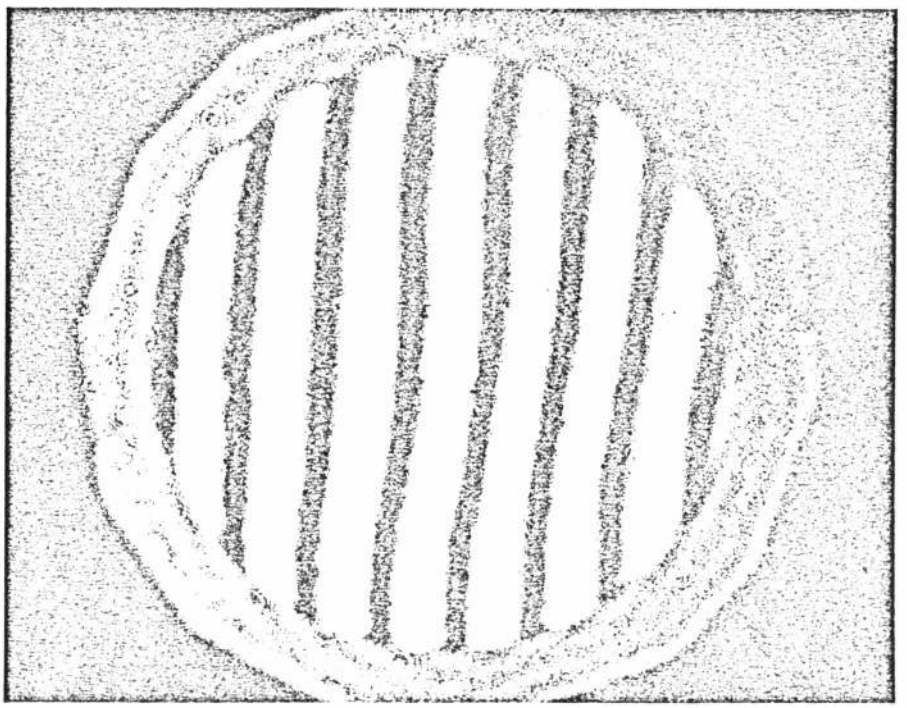

Fig. 23. Interferogram of the same mirror using the zone plate interferometer.

The direction of increasing order of the fringes is the same in both interferograms, which means that since the fringe curvature has the same sense, the indicated error has the same sign. There is obviously close agreement between the figures of the indicated wavefront error introduced by the mirror surface. This result is considered very satisfactory in view of the many possible sources of error, some of which have already been mentioned. A close inspection of the interferograms reveals that there is a difference in fringe curvature, but this is due almost entirely to a slight difference in the setting of the test mirror along the axis. If the difference due to this cause is taken into account, the agreement is remarkably accurate. It is estimated that the remaining difference is not greater than $\lambda/20$. Note the annular zone extending in from the edge by about 0.4 of a radius, and the lack of parallelism between the upper and lower fringes, features which are characteristic of both interferograms.

A further check on the performance of the zone plate interferometer was the testing of a parabolized mirror and an uncoated concave spherical surface, both 15cm diameter. In each case, high contrast fringes were obtained.

4.5 Photographic Distortion

Intentional distortion of the photographic process, by overexposing the film, causes an artificial narrowing of the

fringes of destructive interference. The resultant image of the fringe pattern approaches in appearance that of a multiple-beam interferogram rather than a sinusoidal distribution, revealing small errors in greater detail. But this procedure is effective only if the fringe visibility is very close to unity and the amplitudes of the interfering wavefronts are constant over the field. If these conditions are not fulfilled, the former leads to reduced contrast in the photographic negative and the latter to a variation in the width of the interference fringes - a common defect of interferograms. Fig. 24 is an interferogram obtained with the zone plate interferometer in which the negative was overexposed. There are some localized diffraction patterns across the field associated with scattering specks throughout the system. Except for the presence of these imperfections, the non-linear process could have been continued much further without loss of useful information, and the interferogram illustrates well the high quality of the interference field possible with this interferometer. This is an important point. An interferometer provides a fundamentally simple but extremely accurate method to test optical components. However, many workers fail to appreciate that the potential accuracy of interference measurements is often limited by the quality of the interference pattern. For example, an interferogram substantially free from noise and other imperfections may be electronically analyzed to

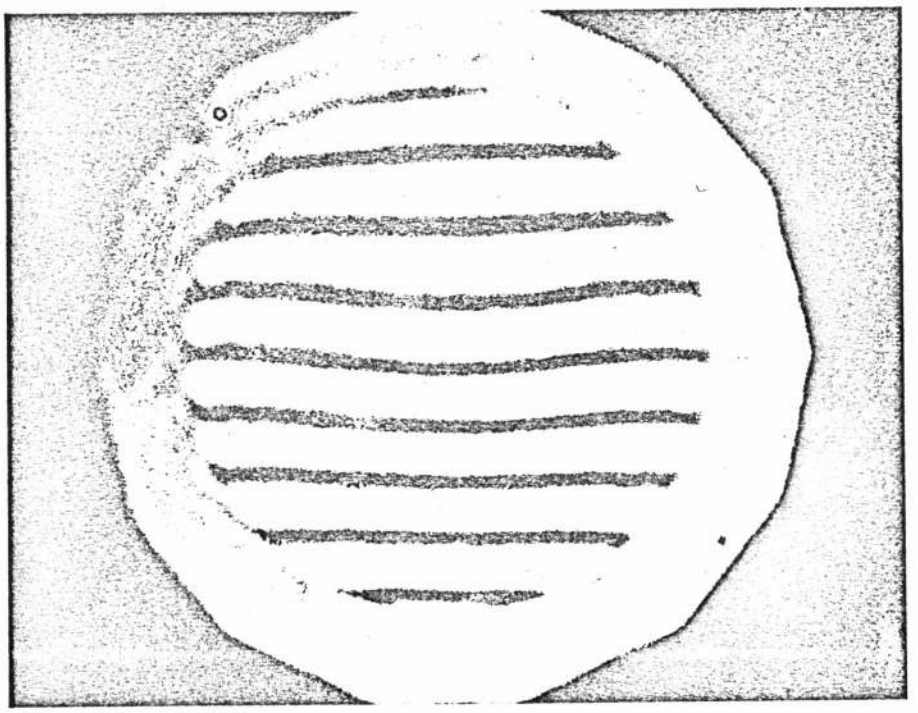

Fig. 24.

Interferogram obtained with the Zone Plate interferometer in which the negative was intentionally overexposed.

locate fringe position to an accuracy of $\lambda/1000$. In more usual cases, a claimed accuracy of $\lambda/20$ would be optimistic.

4.6 Phase of Interferogram

For a centered system, the axial paths are equal, a fundamental property of common-path interferometers. Under these circumstances, the interferogram always has a central constructive interference fringe. The phase of the interferogram may be reversed by adding a small flake of mica, of optical thickness equal to $(2m+1)\ \lambda/4$ (m integral), at the focus of the reference beam on the mirror surface.

V. INTERFEROMETER ERRORS

Sources of possible error in zone plate interferometer measurements will now be considered. It will become evident from the following discussion that this interferometer optical system is to a large measure self-compensating, a property common to some other interferometers. It is largely for this reason that high accuracy in an interferometer test is possible, without the need for a matching accuracy in the interferometer optical components.

5.1 Comparison Between the Three Modes

The three basic modes of the interferometer have been set out in the second chapter. For a convergent reference beam, note that in each case the reference beam wavefront is laterally reversed after reflection; that is, a ray which passes through the zone plate initially at some point will, after reflection at the surface under test, return along a path which intersects the zone plate at a diametrically opposite point (for a centered system). For the test beams however, only in the first mode is the test beam wavefront laterally reversed. In this case the interfering wavefronts have point to point correspondence and common errors cancel. For the second and third modes, the interfering wavefronts are reversed with respect to each other and wavefront errors cancel only when they have radial symmetry. Non-symmetrical errors will thus be registered in the interference pattern.

5.1.1 Wavefront asymmetries

Consider the case of a spherical wave containing an off-axis, localized deformation, incident on the zone plate. For Modes 2 or 3, since only one wavefront is reversed, the error in the reference and test beams due to the deformation will be recorded separately in the interference pattern. An example of this property is illustrated in Figs. 25 and 26 with the interferometer set in the second mode (Fig. 8). A plane-parallel plate has been inserted in the system between the projection lens and the semi-reflector. This plate has a depression, close to spherical, in the center of one surface covering about 3mm diameter with a depth of about 1 wavelength (633nm). In Fig. 25, the plate is not centered in the beam and the interferogram shows the error separately, on one side due to the aberrated test wavefront and on the opposite side the aberrated reference wavefront. When the depression is symmetrical with respect to the optical axis, as indicated in Fig. 26, the error all but disappears from the interferogram, since the wavefronts now match closely, and perfectly so when the deformation is entirely symmetrical.

In practice, even using optics of only moderate optical quality, asymmetrical errors tend to be completely negligible. This is hardly surprising. Characteristically, polishing errors in lenses are rotationally symmetric, and any asymmetry is mostly quite small by comparison. A typical aperture size for the projection lens, the semi-reflector and the zone plate is of the order of 1cm, and

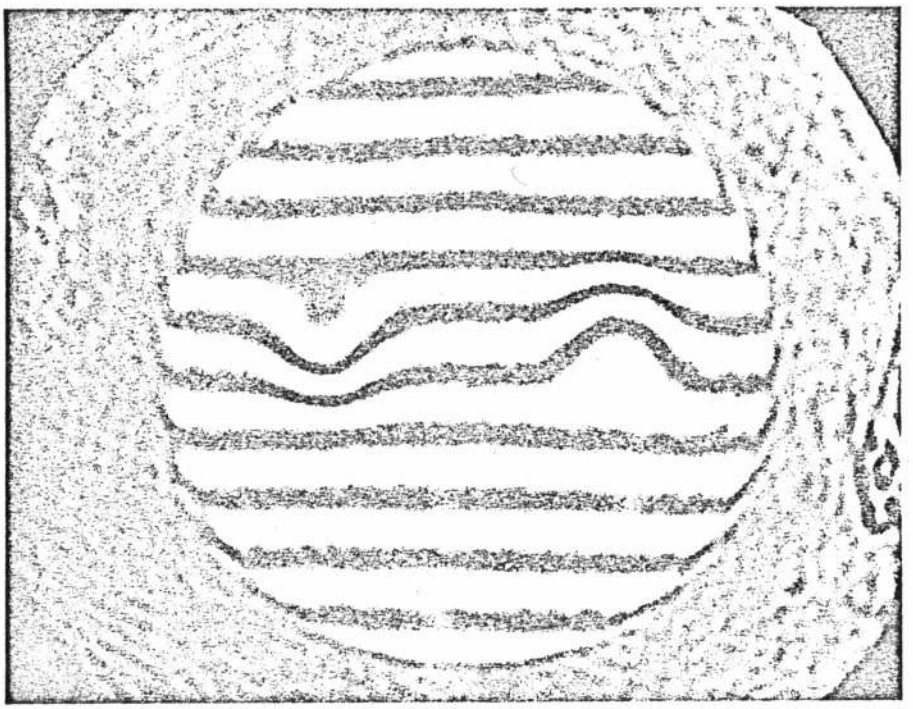

Fig.25. Interferogram in which the incident wavefront has an off-axis, localized deformation.

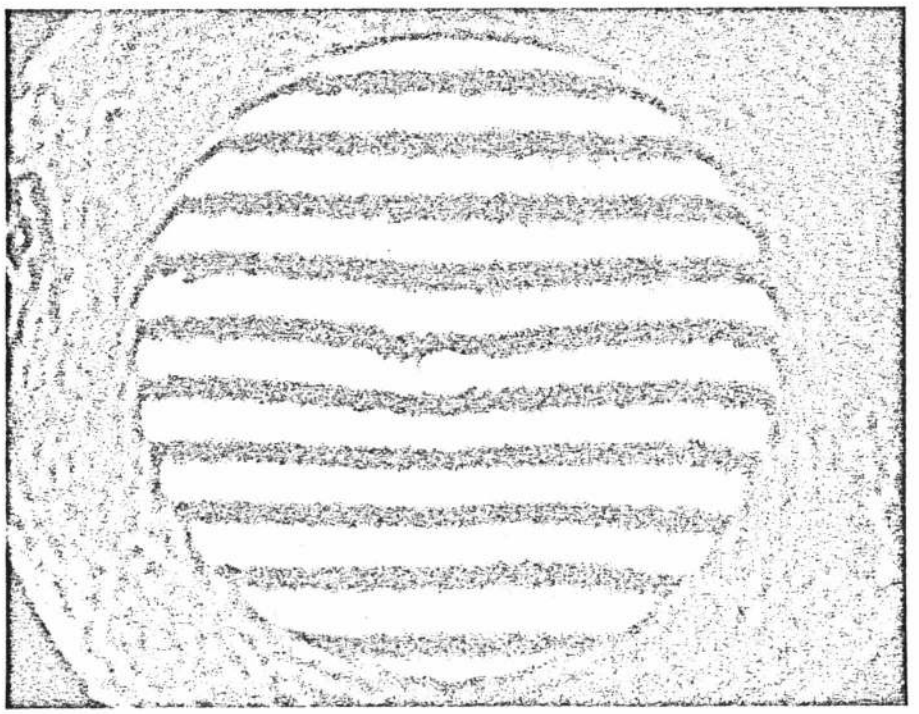

Fig.26. Interferogram in which the incident wavefront has a centered, localized deformation.

if this represents only a small part of the total optical surface in each case, an effective high quality system is likely. We note that for a transmission system, a surface error t contributes only (n-1)t in path difference.

Considerable experience with the use of this interferometer has confirmed this compensating property for symmetrical aberrations. For example, the semi-reflector used was 1cm thick (described in chapter 4), and for an object not at infinity, the wavefront passing through the plate obliquely is distorted by a measurable amount, but this error was never evident in the interference pattern.

The photographic plates on which the zone plates are recorded may however give some trouble. Plates 1mm thick can have quite irregular surface contours, particularly over small, isolated regions. The wavefront error introduced by a zone plate in its performance as an optical window can be measured using one of the standard interferometers. It has been found that most plates have a negligible error (departure from a spherical wavefront) over a 1cm aperture. This is related to the fact that the method of manufacture generally results in a high accuracy of parallelism, with thickness variations far less than surface variations. In any case, correction is simply achieved. Plane cover glasses oiled to each surface of the zone plate entirely remove the effect of such errors. The 6mm thick plates are commonly far more accurate in surface contour and require no correction.

5.2 Zone Plate Alignment

Ideally, for a spherical wave incident on a zone plate, the diffracted wavefronts are also spherical. Misalignment of the zone plate, however, results in distortion of the wavefronts, which can lead to a corresponding error in the interference pattern. In practice, this property of the interferometer presents no problem. Light reflected from the surfaces of the zone plate, for a collimated incident beam, is reimaged in the plane of the source. The zone plate is aligned normal to the optical axis with more than adequate precision when this image is adjusted to be approximately coincident with the source. Moreover, accurate centering of the zone plate is also simply accomplished by centering the multiple foci to some mechanical reference, for example, an iris diaphram. For the reasons cited above, the second and third modes of the interferometer are more sensitive than the first mode to misalignment of the zone plate.

5.3 Zone Plate Aperture

As discussed in Chapter 2, the first mode of the interferometer tests a spherical mirror at the center of curvature strictly only for a vanishingly small zone plate aperture. Scott[8] has discussed in detail a similar configuration for the scatter plate interferometer. He shows that in typical tests, path difference errors associated with off-axis points in the plane of the scatter plate are

completely negligible. Note that the second and third modes test truly at the center of curvature.

5.4 Reference Beam Focus

For the first version of each of the three modes, the reference beam forms an image of the source at the test surface. We now consider qualitatively the change in the interference pattern as the location of the image is shifted along the axis from the surface; that is, the case of an inexact setting of the reference beam focus. The location of this focus is controlled by the setting of the lens L_1 (Fig.20). For a spherical mirror set with zero tilt, the number of circular fringes in the interference field varies as the focus shifts, due to the resultant difference in curvature of the reference and test wavefronts in the region of interference. For small shifts, this is entirely equivalent to an adjustment where the reference beam is precisely focused at the test surface, while the test beam wavefront is changed in curvature by varying the distance between the test surface and zone plate. This is equivalent, in turn, to the usual two-beam interferometer focus adjustment. We conclude therefore that focusing of the reference beam is not critical.

5.5 Spherical Aberration

The third order aberrations of a Fresnel zone plate, considered as a focusing device, have been studied by Kamiya[18]. He used Fermat's principle as the most general

approach to such an analysis.

Note that for a grating such as the zone plate, the condition for the forming of an image is that the optical path difference between a central ray and a ray passing through the jth aperture should be $mj\lambda$, where m is the order number and j=0,1,2,...

Kamiya[18] has obtained expressions for spherical aberration, coma, astigmatism, and field curvature, with distortion zero. He takes the radii of the transmitting apertures of the zone plate as being proportional to the square roots of consecutive integers. He points out that for such a specification, that is where the radii are slightly shorter than for the exact case, a collimated beam incident on the zone plate will fail to form a perfect focus. However, for zone plates prepared as described in Chapter 3, a'perfect' focus is formed when the zone plate is illuminated with a collimated beam. For all other positions of an on-axis object point, except where it coincides with a focus of the zone plate, spherical aberration of the image occurs.

It is simplest to consider the affect of this aberration on the performance of the interferometer from simple physical principles. A conjugate relationship exists between the plus and minus order foci of a zone plate. Hence, to a first approximation, the angular error associated with an aberrated ray is equal in magnitude for conjugate beams - and it is conjugate beams which interfere in the interferometer. Hence the reference and test beams contain the same

error, and this error will therefore not appear in the interference pattern. That is, the interferometer is self-compensating for symmetrical aberrations generated by the zone plate.

SUMMARY

The description of a Fresnel zone plate interferometer given elsewhere is not a unique configuration for this interferometer. It has been shown here, based on the properties of a zone plate, that a number of other configurations are possible. To provide further understanding of the operation of this interferometer, it has been pointed out also that a compound interference pattern can be identified with each of these configurations.

The developed form of this interferometer has been described in detail. Aspects of this work which have been emphasized are the manufacture of 'fast' zone plates photographically, and their use in the form of compensated phase zone plates which results in high transmittance and the generation of uniform amplitude wavefronts.

The practicality of this form of the zone plate interferometer has been demonstrated and illustrated by a simple comparison with the Twyman-Green interferometer. Particular features of this instrument have also been stressed, such as a means to eliminate extraneous light from the interference pattern (a typical problem associated with common-path interferometers), the possibility to test a concave mirror at f/0.5, and interference fringes with close to unit visibility.

BIBLIOGRAPHY

1. M.V.R.K. Murty, J. Opt. Soc. Am. 53, 568 (1963).
2. J.M.Burch, Nature 171, 889 (1953).
3. U/R Int. Tech. Report (4), Opt. Tech. Prog., AF 33-615-3777 (1967).
4. W.J.Bates. Proc. Phys. Soc. 59, 940 (1947)
5. J. Dyson, Concepts of Classical Optics (J. Strong). Appendix B, San Francisco, Freeman (1958).
6. W.H.Steel, Interferometry, Cambridge University Press (1967).
7. J. Dyson, J. Opt. Soc. Am. 47, 386 (1957).
8. R.M.Scott, Appl. Opt. 8, 531 (1969).
9. R.W.Wood, Phil. Mag. 45, 511 (1898).
10. H.H.M. Chau, Appl. Opt. 8, 1209 (1969).
11. R.N.Smartt, Appl. Opt. 9, 970 (1970).
12. J. Upatnieks, C. Leonard, Appl. Opt. 8, 85 (1969).
13. N. George, J.W. Matthews, Appl. Phys. Letters 9 (1966).
14. J.H. Altman, Appl. Opt. 5, 1689 (1966).
15. H.M.Smith, J. Opt. Soc. Am. 58, 533 (1968).
16. G. Oster, M. Wasserman, C. Zweling, J. Opt. Soc. Am. 54, 169 (1964).
17. G. Oster, Modern Optics, 541, New York, Polytechnic Press (1967).
18. K. Kamiya, Science of Light, 12, 35 (1963).